https://doi.org/10.5194/egusphere-2023-570
Preprint. Discussion started: 11 April 2023

Two-year measurements of Black Carbon properties at the high-altitude mountain site of Pic du Midi Observatory in the French Pyrenees

Sarah Tinorua[1], Cyrielle Denjean[1], Pierre Nabat[1], Thierry Bourrianne[1], Véronique Pont[2], François Gheusi[2], and Emmanuel Leclerc[2]

[1]CNRM, Université de Toulouse, Météo-France, CNRS, Toulouse, France
[2]Laboratoire d'Aérologie, UPS Université Toulouse 3, CNRS (UMR 5560), Toulouse, France

Correspondence: Sarah Tinorua (sarah.tinorua@meteo.fr), Cyrielle Denjean (cyrielle.denjean@meteo.fr)

Abstract. Black Carbon containing particles (BC) are strong light absorbers, causing substantial radiative heating of the atmosphere. The climate-relevant properties of BC are poorly constrained in high-elevation mountain regions, where numerous complex interactions between BC, radiation, clouds and snow have important climate implications. This study presents two-year measurements of BC microphysical and optical properties at the research station of Pic du Midi (PDM), a high-altitude observatory located at 2877 m above sea level in the French Pyrenees. Among the worldwide existing long-term monitoring sites, PDM has experiences limited influence of the planetary boundary layer (PBL), making it an appropriate site for characterizing free tropospheric (FT) BC. The classification of the dominant aerosol type using the spectral optical properties of the aerosols indicates that BC was the predominant absorption component of aerosols at PDM and controlled the variation of Single Scattering Albedo (SSA) throughout the two years. Single-particle soot photometer (SP2) measurements showed a mean mass concentrations of BC (M_{BC}) of 35 ng m^{-3} and a relatively constant BC core mass-equivalent diameter of around 180 nm, which are typical values for remote mountain sites. Combining the M_{BC} with in situ absorption measurements yielded a BC mass absorption coefficient (MAC_{BC}) of 9.8 $\pm$ 2.7 m^2 g^{-1} at 880 nm, which corresponds to an absorption enhancement (E_{abs}) of 2.4 compared to that of bare BC particles with equal BC core size distribution. A significant reduction of the ratio $\Delta BC/\Delta CO$ when precipitation occurred along the air mass transport suggests wet removal of BC. However we found that the wet removal process did not affect the size of BC, resulting in unchanged E_{abs}. We observed a large seasonal contrast in BC properties with higher M_{BC} and E_{abs} in summer than winter. In winter a strong diurnal variability of M_{BC} (E_{abs}) with higher (lower) values in the middle of the day was linked to the injection of BC originating from the PBL. During summer in contrast, M_{BC} showed no diurnal variation was rather constant despite more frequent PBL-conditions, implying that M_{BC} fluctuations were rather dominated by regional and long-range transport in the FT. A body of evidence suggests that biomass burning emissions effectively altered the concentration and optical properties of BC at PDM, leading to higher E_{abs} in summer compared to winter. The diurnal pattern of E_{abs} in summer was opposite to that observed in winter with maximum values of 2.9 observed at noon. We suggest that this daily variation results from photochemical processing driving BC mixing state rather than a change in BC emission source.

https://doi.org/10.5194/egusphere-2023-570
Preprint. Discussion started: 11 April 2023

Such direct two-year observations of BC properties provide quantitative constraints for both regional and global climate models and have the potential to close the gap between model predicted and observed effects of BC on regional radiation budget and climate. The results demonstrates the complex influence of BC emission sources, transport pathways, atmospheric dynamics and chemical reactivity in driving the light absorption of BC.

1 Introduction

Black Carbon (BC) is a light-absorbing carbonaceous aerosol produced by incomplete combustion of fossil fuels and biomass. This includes anthropogenic emissions from traffic, residential heating and cooking, power plants, industries, but also natural emissions such as biomass burning (Bond et al., 2013; Bond and Bergstrom, 2006). Recent scientific assessments of the 6th IPCC (Intergovernmental Panel on Climate Change) report (Szopa et al., 2021b) estimates that BC is the most absorbing atmospheric aerosol with a best estimate of effective radiative forcing of around +0.107 W m^{-2} , thereby increasing the global mean surface air temperature by 0.063 °C for the period 1750–2019 (Szopa et al., 2021a). The contribution of BC to climate change is estimated to have highest uncertainty ($\sim$90%) in climate models, limiting their accuracy (Bellouin et al., 2020). The large uncertainty of BC direct radiative forcing due to BC-radiation interactions can be attributed, in addition to uncertainties in BC emissions and lifetime, to variations of its optical properties that are neglected by climate models.

A crucial factor for estimating the BC radiative effect is the mass absorption cross-section (MAC_{BC}), which is defined as the light absorption-equivalent cross-section of BC per unit of mass concentration (M_{BC}). Observations show that the BC radiative forcing is likely underestimated by about 10-40% in current climate models due to too low simulated MAC_{BC} (Bond et al., 2013; Boucher et al., 2016; Matsui et al., 2018; Myhre and Samset, 2015). In-situ measurements of MAC_{BC} reported a wide range of values, going from 3.8 m^2 g^{-1} to 58 m^2 g^{-1} (Wei et al., 2020). Although such high variability can be attributed, in part, to the determination method of the MAC_{BC} based on M_{BC} and absorption measurement techniques, differences in MAC_{BC} values were found even for the same measurement technique. Values of MAC_{BC} depend on BC microphysical and chemical properties, which are related to their emission sources (Schwarz et al., 2008) and the effects of aging processes during the transport in the atmosphere (Ko et al., 2020; Laborde et al., 2013; Sedlacek et al., 2022). Freshly emitted BC is made of porous, fractal-like aggregates of nanoparticles (Beeler and Chakrabarty, 2022; China et al., 2013) that can become coated by condensation and/or coagulation with non-BC components (such as sulfate, nitrate, and organic components) during atmospheric aging (Fierce et al., 2020). Conversely this coating can be removed through evaporation and/or chemical processing via the production of more volatile substances (Sedlacek et al., 2022). Numerous studies have demonstrated that coating of BC with non-absorbing materials is accompanied by an enhancement of light absorption (E_{abs}) through the so-called lensing effect (Cappa et al., 2012; Denjean et al., 2020; Healy et al., 2015; Liu et al., 2015; McMeeking et al., 2014; Peng et al., 2016; Van de Hulst, 1957; Xie et al., 2019; Schwarz et al., 2006; Yus-Díez et al., 2022). However, most of these measurements were performed in the Planetary Boundary Layer (PBL) and over short periods.

Both observations and model simulations pointed out an amplification of the warming rate by greenhouse gases and absorbing aerosols at high-mountain sites compared to PBL areas (Gao et al., 2018; Liu et al., 2009; Pepin et al., 2019; Rangwala,

https://doi.org/10.5194/egusphere-2023-570
Preprint. Discussion started: 11 April 2023

2013). López-Moreno et al. (2014) found a positive trend between altitude and warming rate in the Spanish Pyrenees , which could lead to the occurrence of warm events multiplied by two between 2021-2050 and even more until 2080. This so-called Elevation dependent warming (EDW) has been reviewed by the Mountain Research Initiative EDW Working Group, 2015, who listed the possible mechanisms of this phenomenon (Pepin et al., 2015). Among the invoked reasons, BC is a potential driver of EDW by affecting both absorbing solar radiation in the troposphere and decreasing the surface albedo when deposited on the cryosphere, thereby accelerating snowmelt (Réveillet et al., 2022). In addition, BC was found to have a higher radiative effect when it is located above clouds rather than near the surface (Samset and Myhre, 2015; Sanroma et al., 2010). All these findings highlight the importance of studying BC at high altitude mountain sites, where its effects on climate could be even more significant.

This study presents two-year continuous measurements of BC and aerosol properties at the high-altitude long-term monitoring station Pic du Midi (PDM). Located at 2877 m above sea level (asl) in the French Pyrenees, PDM has been early identified as a clean remote station (Marenco et al., 1994). By means of a backward particle dispersion model, Henne et al. (2010) found the influence of local anthropogenic emissions to be very limited at PDM, and classified the station in the "mostly remote" category. Collaud Coen et al. (2018) defined an "ABL-Topoindex" as a metrics of the atmospheric boundary layer influence for a mountain site. PDM was found to have a low ABL-Topoindex, similar to other Alpine high altitude stations. PDM is thus a suitable site to study both the background lower free troposphere (FT) over long timescales and injection of air masses from the PBL (Hulin et al., 2019; Tsamalis et al., 2014; Fu et al., 2016; Marusczak et al., 2017). In this article the instrumentation and methodology are presented in section 2. Section 3 presents the results of the measurement campaign including the meteorology and air mass origin, the aerosol optical properties and black carbon properties. In Section 4, the possible factors influencing the variability of E_{abs} are discussed.

2 Methods

2.1 Measurement site and observation period

Measurements were performed at the mountain research station Pic du Midi (PDM, 42°56'11" N, 0°08'34" E, 2877 m. above sea level) in the French Pyrenees. This station is part of the Pyrenean Platform for Observation of the Atmosphere (P2OA)[1]. As shown in Fig. 1, the site is located 150 km east of the Atlantic coast. The high isolated summit is shifted about 20 km north of the main Pyrenean crest (France-Spain border) and thus, closely dominates the French plain. Long-term monitoring of extensive meteorological, gas and aerosol parameters have been conducted for mostly two decades, notably through the Global Atmospheric Watch (GAW) program of the World Meteorological Organization (WMO), as well as the national research infrastructure ACTRIS-France. Results from the Hygroscopic properties of Black Carbon (h-BC) campaign performed from February 2019 to January 2021 at PDM (in addition to the routine measurements) are presented in this paper.

[1] http://p2oa.aeris-data.fr

https://doi.org/10.5194/egusphere-2023-570
Preprint. Discussion started: 11 April 2023

Figure 1. Geographical location of the Pic du Midi Observatory in the French Pyrenees (© Google Earth).

2.2 Instrumentation

2.2.1 Total inlet

All particle-measuring instruments were sampling air drawn in parallel from a Whole Air Inlet, which is utilized for the long-term observations and sucked air 2 m above the building roof. Air was heated to ≈20°C in order to keep the relative humidity below 20% (Nessler et al., 2003).

2.2.2 Black carbon measurements

M_{BC} and BC size distribution were measured by a Single Particle Soot Photometer (SP2, Droplet Measurement Technology, Boulder, USA). Its operating principles have been described in previous articles (Gao et al., 2007; Moteki and Kondo, 2007; Schwarz et al., 2006). In short, this instrument uses a laser-induced incandescence technique which quantifies BC mass in single particles. A continuous intracavity laser beam (Nd:YAG; λ=1064 nm) is used to heat BC-containing particles to their vaporization point. The measured incandescence signal of an individual BC-containing particle can be converted to a BC mass, which was calibrated using mobility size-selected fullerene soot particles (Alfa Aesar, lot #FS12S011) and assuming BC mass density of 1.8 g cm^{-3}. This calibration was performed twice a year and did not evolve thorough the two-year measurement campaign. The SP2 data were processed using a Python code following the method used in the SP2 Toolkit from the Paul Scherer Institute (Gysel et al., 2009). The SP2 used in this study measured BC cores over a size range between 90 and 580 nm. The observed size distributions showed an increase in M_{BC} at diameters less than 90 nm (Figure S1 in the Supplement).

https://doi.org/10.5194/egusphere-2023-570
Preprint. Discussion started: 11 April 2023

Because of these small-mode particles below the SP2 detection window, the SP2 M_{BC} measurements could be underestimated. To compensate the missing mass the observed BC size distributions have been fitted using the sum of three individual lognormal distribution to extrapolate BC size distribution in the range 10 to 1000 nm. The position of the three modes were constrained in the following ranges : Mode 1 : $50 < d_g < 100$ nm and $1.2 < \sigma_g < 3$; Mode 2 : $150 < d_g < 250$ nm and $1.3 < \sigma_g < 2.9$; Mode 3 : $350 < d_g < 500$ nm and $1 < \sigma_g < 3$. Using the fitting procedure, a time-dependent missing mass correction was applied to the observed M_{BC} to calculate to overall M_{BC}. The missing mass correction factor applied over the campaign was 1.2 ± 1.1 (Mean value $\pm$ STD). The extent to which uncertainty in this fitting procedure contribute to the overall M_{BC} was quantified by comparing the M_{BC} calculated from the observed BC size distribution and the fit curve over the SP2 size range. An excellent match was obtained between the measured and fitted size distribution, resulting in differences by less than 0.2 %. The combined uncertainty on the M_{BC} was estimated to be about 24.5 % by calculating the quadratic sum of measurement uncertainties on sampling flow, anisokinetic sampling errors, and missing mass correction factor.

2.2.3 Aerosol properties

A Scanning Mobility Particle Sizer (SMPS), combining a differential mobility analyzer (DMA, TSI 3071) and a CPC (TSI 3772) allows the determination of aerosols size distribution between 12.6 nm and 532.6 nm.

Aerosols scattering coefficients (σ_{sca}) at three wavelengths (450 nm, 525 nm, 635 nm) were measured with an integrating nephelometer (model Aurora 3000, Ecotech Pty Ltd, Knoxfield, Australia). A calibration with carbon dioxide and filtered air was performed every three months. The instrument measures σ_{sca} in the angular range 10-170°, and the correction of Müller et al. (2011) was used to account for the angular truncation errors.

Aerosol absorption coefficients (σ_{ap}) were measured by a seven-wavelength aethalometer (model AE33, Magee Scientific Company, Berkeley, USA). This instrument measures light attenuation through a filter on which aerosol sample is deposited. The aethalometer filter loading effect was corrected online by the dual-spot manufacturer correction proposed by Drinovec et al. (2015). The multiple scattering artifact was corrected using a C value of 3.63, as obtained by Tinorua et al. (2023, in preparation). Uncertainty on the corrected σ_{ap} were estimated to be 35 % (Zanatta et al., 2016). The detection limit of the aethalometer is 0.005 μg m^{-3} of M_{BC}, which corresponds to 0.0215 Mm^{-1} in absorption. Values under this low limit were filtered out before the analysis.

2.2.4 Gas-phase measurements

Two different instruments, have been deployed to measure carbon monoxide (CO) with a final 1-h time resolution: an IR-absorption analyser (TEI 48CTL) placed close to the aerosol instrumentation in order to detect pollution plumes produced locally at PDM[2] (hourly CO concentrations above 200 ppb were filtered out), and a Cavity Ring Down Spectrometer (CRDS Picarro model G2401), located in an other building, used to measure the background carbon monoxide (CO) concentration and calculate $\Delta BC/\Delta CO$ ratios.

[2]e.g. due to snow removal of the touristic platform

https://doi.org/10.5194/egusphere-2023-570
Preprint. Discussion started: 11 April 2023

A key issue in our study is the distinction between FT and PBL-influenced air masses. Optical properties of BC depends on its aging and transport pathways in the atmosphere, so that it is crucial to determine whether it has been transported over the BL or in the FT. For this purpose, we routinely monitor the diurnal cycle of radon (^{222}Rn) volumic activity (in mBq m^{-3}) at PDM with a 1500-L high-sensitivity radon monitor manufactured by ANSTO (Whittlestone and Zahorowski, 1998). Radon is an inert radioactive gas emitted from ice-free soils with a half-life of 3.8 days, making it the most reliable tracer to discriminate between the FT and PBL- influenced air masses (Chambers et al., 2013).

2.3 Determination of intensive aerosol and BC properties

The spectral dependence of σ_{ap} was characterized by the Absorption Ångström Exponent ($AAE_{aer,450\text{-}635}$) as :

$$AAE_{aer,450-635} = \frac{-log\left(\frac{\sigma_{ap,450}}{\sigma_{ap,635}}\right)}{\left(\frac{log(450)}{log(635)}\right)} \quad (1)$$

Here the $AAE_{aer,450\text{-}635}$ was calculated between the wavelengths of 450 and 635 nm. To do so, $\sigma_{ap,\,635}$ was first calculated using the $AAE_{aer,590\text{-}660}$. The wavelength dependence of σ_{sca} can be characterized by the Scattering Ångström Exponent ($SAE_{aer,450\text{-}635}$) calculated between 450 and 635 nm,as :

$$SAE_{aer,450-635} = \frac{-log\left(\frac{\sigma_{sca,450}}{\sigma_{sca,635}}\right)}{\left(\frac{log(450)}{log(635)}\right)} \quad (2)$$

The aerosols Single Scattering Albedo (SSA_{aer}) was calculated at the wavelengths of 450, 525 and 635 nm using the following equation :

$$SSA_{aer,\lambda} = \frac{\sigma_{sca,\lambda}}{\sigma_{sca,\lambda} + \sigma_{ap,\lambda}} \quad (3)$$

For that purpose, σ_{ap} was first calculated at the proper wavelengths λ using the AAE calculated at the closest wavelengths ($AAE_{aer,370\text{-}470}$ to retrieve $\sigma_{ap,450}$, $AAE_{aer,520\text{-}590}$ for the $\sigma_{ap,525}$, and $AAE_{aer,590\text{-}660}$ for the $\sigma_{ap,635}$). $\Delta BC/\Delta CO$ emission ratio was calculated to provide information on the combustion sources, as well as on meteorological conditions (Baumgardner et al., 2002). First, the background CO concentrations were estimated by taking the rolling 5th percentile of the values on a 14-day time window and then calculating a monthly mean (see fig S2 in the Supplement) based on the method by Kanaya et al. (2016). ΔCO was then calculated by subtracting the monthly background CO concentration to any measured hourly CO value. ΔBC was taken to be equal to M_{BC}, because we assume that the background BC is zero since the atmospheric lifetime of BC is known to be of a few days, which is much smaller than CO lifetime (1 or 2 months). The Mass Absorption cross-section of BC (MAC_{BC}) was determined as :

$$MAC_{BC} = \frac{\sigma_{ap,880}}{M_{BC}} \quad (4)$$

https://doi.org/10.5194/egusphere-2023-570
Preprint. Discussion started: 11 April 2023

M_{BC} under (resp. over) the 5th (resp. 95th) percentile were filtered before MAC calculations to reduce the influence of outliers in statistical analyses. As shown in Tinorua et al . (2023, in preparation), the presence of dust can lead to strong overestimation of $\sigma_{ap,880}$. Therefore periods with dust sampled at PDM were eliminated before the MAC_{BC} calculations following the method presented in section 3.2.

The light-absorption enhancement factor E_{abs} can be determined as the MAC_{BC} values normalized by a reference value for pure, uncoated (bare) BC:

$$E_{abs} = \frac{MAC_{BC}}{MAC_{bare,BC}} \tag{5}$$

Three different methods are usually used to estimate $MAC_{bare,BC}$: the first one is to remove the coating of BC with a thermodenuder and measure the corresponding absorption; the second one is to extrapolate measurements of MAC_{BC} as a function of the measured BC mixing ratio; and the third one consists in calculating $MAC_{bare,BC}$ from the measured BC size distribution using Mie theory and the mean geometric BC diameter (see fig. S3 in the Supplement). Here we used this latest method by assuming a BC refractive index of 1,95 - 0.79i at λ=880 nm (Bond and Bergstrom, 2006).

Time periods with high humidity (95%) or precipitations were filtered before analysis to avoid artifacts in the sampling inlet. We also filtered periods where hourly CO concentrations exceeded 200 ppb in order to exclude local pollution events.

All aerosol and gas measurements were converted to standard temperature and pressure (273.15 K and 101.325 hPa).

2.4 Identification of air mass origins

The Hybrid Single Particle Lagrangian Integrated Trajectory Model (HYSPLIT) (Draxler and Hess, 1997) was used to calculate air masses backtrajectories. This model uses 3-hourly atmospheric data from the Global Data Assimilation System (GDAS) of the National Center for Environmental Prediction (NCEP) in a 1°×1° spatial resolution. More information can be found on https://www.ready.noaa.gov/index.php. One backtrajectory was run every 24h going 72h back in time at 12h for the two-year period of the campaign. Every backtrajectory arrived at the PDM altitude and coordinates. Precipitation rates along the back trajectories were also computed from the HYSPLIT calculations, in order to classify days where the air masses arriving at PDM encountered precipitations or not in the past 72h.

To discriminate FT and PBL-influenced air masses, we followed the methodology proposed initially by Griffiths et al. (2014) assuming that the diurnal radon increase, which is often observed at mountain sites during the daytime, is the result of transport of PBL air by thermal anabatic winds up to the summits. The method first consists in ranking each day of the sampling period by decreasing anabatic influence (no details on the iterative ranking process are given here, but can be found in Griffiths et al. (2014)). Then, a value called "anabatic radon" can be calculated for each day, which represents (in short) the average deviation of radon volumic activity above a nocturnal background (see again details in Griffiths et al. (2014)). Anabatic radon mostly decreases with increasing anabatic rank (Fig. S4 of the Supplement), at least up to a threshold rank (282) corresponding to the absolute minimum of anabatic radon. After this rank, the radon variations are no more in phase with the diurnal thermal cycle, and may be due to any other causes than anabatic transport[3]. For this reason, the threshold rank can be used to separate

[3]By construction, a value of "anabatic" radon can still be calculated but actually makes no more sense, explaining the random fluctuations after rank 282.

https://doi.org/10.5194/egusphere-2023-570
Preprint. Discussion started: 11 April 2023

anabatically-influenced days from non influenced days. In the present study, when we needed to select hours with strong influence of the boundary layer, we chose, among the 200 first days in the ranking the hours when the radon activity was higher than the daily median value. Conversely, hours without influence of PBL are selected among days after the rank 282, when the radon activity was under the daily median value.

3 Results

3.1 Meteorology and air mass classification

The meteorological conditions at PDM during the campaign were characterized by a strong seasonal trend of temperatures, with daily means ranging between -15 and +15°C (Figure 2). The time series of relative humidity (RH) covered a wide range between 5% and 100% with an annual mean value of 71.2 %. Lower ambient RH was observed in summer compared to winter with median values of 67% and 78%, respectively. Irrespective of the season, the wind direction was dominated by westerly and south-westerly winds and a median speed of 7 m.s^{-1}.

The backward trajectories performed with the HYSPLIT model on 72h-periods of time were assigned to six geographical zones, according to the position of their start point (shown in Figure 3): North-west Europe, Continental Europe, Med-Africa, Atlantic Spain, North Atlantic and Local (within a circular zone of 100 km radius around PDM). Transport to PDM was generally westerly or southerly, from the Atlantic Ocean towards North America or the Iberian Peninsula. It can also be noticed that 99% of all atmospheric backward trajectories modelled to PDM reveal long-range transport (>100 km).

The analyses of the diurnal cycle of radon concentrations allowed to determine the FT- and PBL-influenced conditions prevailing at the site following the methodology presented in Section 2.5. Details on the statistical results can be found in Table S1 in the Supplement. Over the campaign, 1149 hours were clearly identified as FT-influenced conditions, which represents 56% of the total classified hours. In winter, FT- and PBL-influenced conditions occurred roughly 74% and 26% of the analyzed time, respectively, against 48% and 52% for summer, respectively. These results are broadly in agreement with the previous study by Hulin et al. (2019) at PDM, which quantified around 47 % of the days as PBL-influenced over a 10 years period. The PBL-influenced coditions occured mostly around 15:00 UTC, consistent with the dynamics at mountain sites where plain-to-mountain winds and along-valley winds become the strongest in the afternoon (Whiteman, 2000).

3.2 Aerosol optical properties and classification of aerosol types

Figure 4 presents daily time series and statistics of aerosol optical properties over the two-year measurement period. The average SSA ± GSD were 0.94 ± 0.06, 0.94 ± 0.07 and 0.95 ± 0.08 at 450, 525 and 635 nm, respectively (Figure 4a). These values are in the range of those observed at mountain sites in Southern Europe (Bukowiecki et al., 2016; Laj et al., 2020; Pandolfi et al., 2014). The mean value ± GSD of $\sigma_{ap,880}$ was 0.27 ± 0.25 Mm^{-1}, which falls in the range of 0.14 to 1.23 Mm^{-1} obtained at Jungfraujoch and Montsec (Bukowiecki et al., 2016; Pandolfi et al., 2014). These weak values can be explained by the remote mountain site type, where almost no absorbing aerosols are locally emitted. There was a clear seasonality of

https://doi.org/10.5194/egusphere-2023-570
Preprint. Discussion started: 11 April 2023

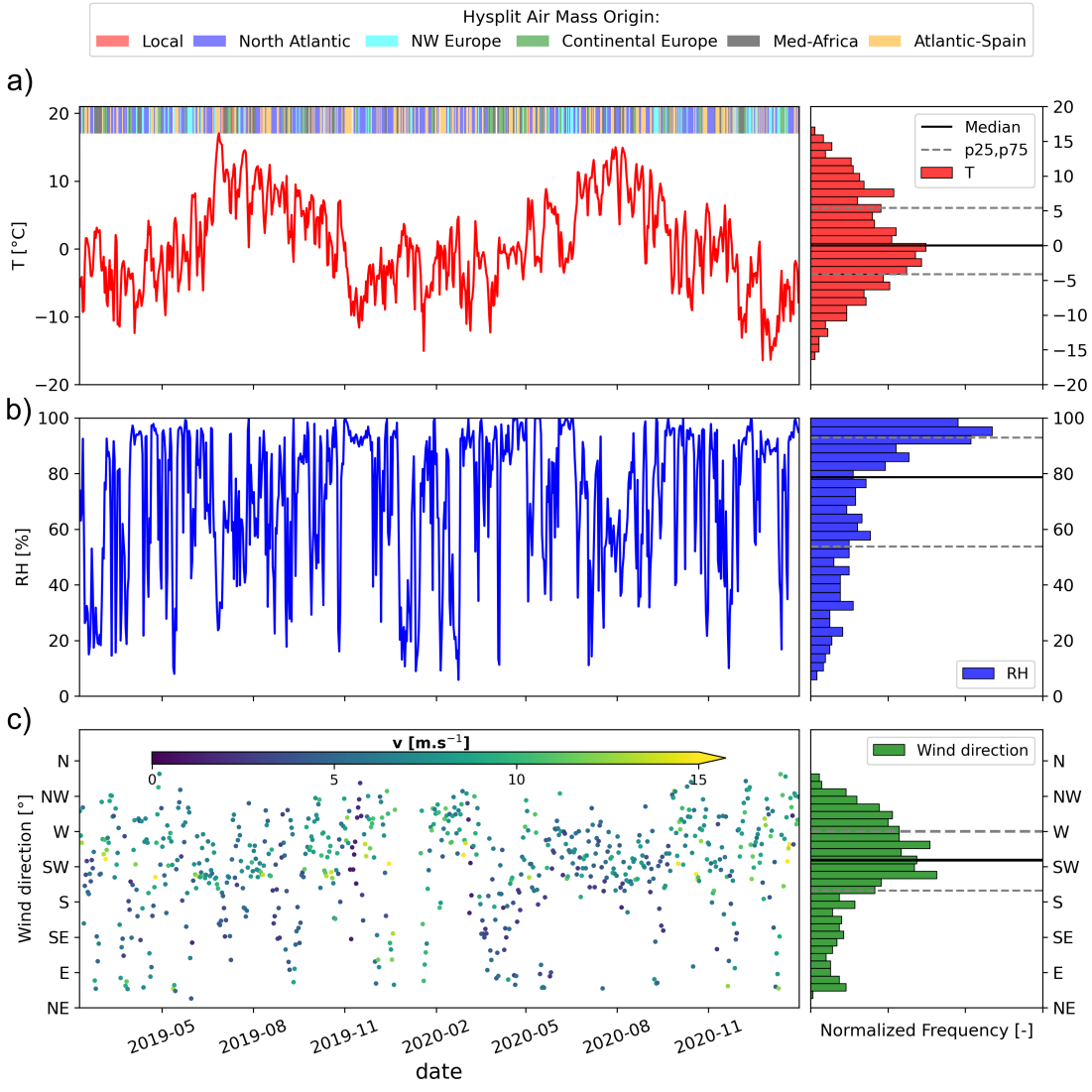

Figure 2. Time series (left) and statistical distributions (median, 25th and 75th percentiles, right) of meteorological parameters measured at PDM in 2019-2020 with (a) the temperature and Hysplit air mass origin, (b) the relative humidity and (c) the wind direction and speed. Daily average data are shown.

SSA with a minimum around 0.93 during spring-summer and higher values around 0.97 in autumn-winter. Simultaneously, both SAE and $\sigma_{ap,880}$ increased by a factor 2 and 5, respectively, during spring-summer compared to autumn-winter, thus suggesting a higher influence of absorbing fine particles at PDM during the warmest months (Figures 4b-d). Figure 4c shows a less pronounced AAE seasonal variation (1.13 ± 0.35), indicating a rather constant composition of absorbing aerosol particles. This noteworthy annual seasonality of aerosol optical properties has previously been observed at other high mountain sites

https://doi.org/10.5194/egusphere-2023-570
Preprint. Discussion started: 11 April 2023

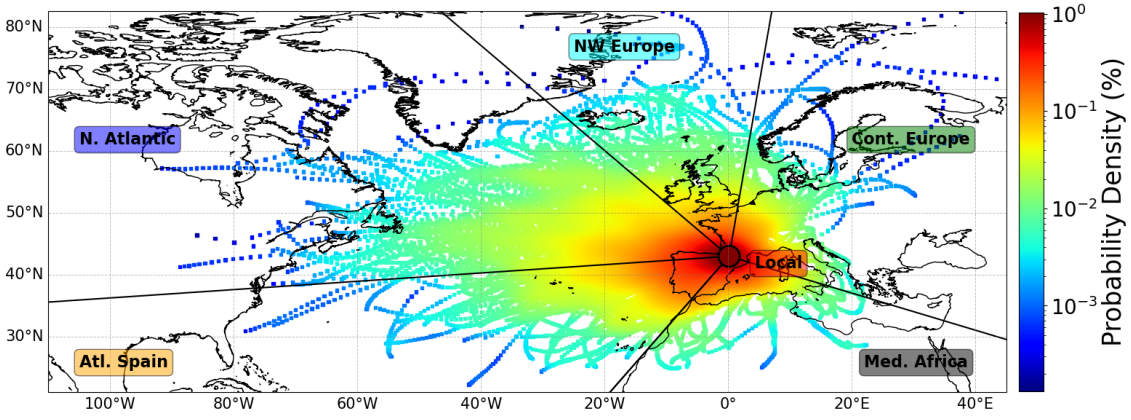

Figure 3. 72-h Back trajectories of air masses measured at PDM over the measurement period 2019-2020. Geographical boundaries of the sectors used to classify the air mass back-trajectories are overlaid.

in Europe (Andrews et al., 2011; Collaud Coen et al., 2011; Laj et al., 2020; Pandolfi et al., 2018). It has been attributed to the seasonal variation of the continental boundary layer height, long-range transport events (e.g. Saharan dust outbreaks, coal burning from eastern Europe) and biomass burning both from forest fires in summer and domestic heating in winter.

A classification of the dominant aerosol type sampled at PDM was performed by using the spectral aerosol optical properties. Figure 5 shows AAE as a function of SAE, overlaid with the aerosol classification matrix from Cappa et al. (2016). Aerosol with the highest SSA values (violet points) tend to fall on the left-hand side of the plot with SAE values below 0, indicative of large particles such as marine sea salt, continental dust or highly processed/coated particles. The presence of large marine and dust aerosol is in line with backward trajectories showing a dominant origin of air masses coming from the Atlantic Ocean and Iberian Peninsula as far as North Africa (e.g. Figure 3). Dust being a strong light absorber, it is expected to lower the mean aerosol SSA. However Figure 5 shows that SSA for dust-dominated aerosol (classified as having AAE values above 2) are quite similar as those for remote marine aerosol (classified AAE values below 1). Although Europe frequently experiences African dust events (Denjean et al., 2016; Dumont et al., 2023) , our results indicate that these dust events were not absorbing enough to substantially lower the aerosol SSA at PDM. This is supported by previous estimates of SSA ranging between 0.90–1.00 for dust particles transported in the Mediterranean region (Mallet et al., 2013; Denjean et al., 2016).

There was a natural clustering of the most light absorbing aerosols with SSA<0.9 (pink to yellow points) on the middle of the plot, with sections on the lower side with AAE between 0.5 and 1.5, which Cappa et al. (2016) defined as dominated by BC or mixed with BC with large particles the sections. The success of aerosol classification schemes is largely dependent on uncertainties in AAE attribution for each aerosol species. Although AAE = 1 is often considered for BC such as that in the classification by Cappa et al. (2016), observational and numerical estimates show a wide range of BC AAE from 0.6 to 1.3 (Kirchstetter et al., 2004; Liu et al., 2018) due to the variation of BC core size, coating thickness, composition and morphology (Liu et al., 2018; Zhang et al., 2018). Therefore it is possible that the large range of AAE values observed for the most light-absorbing aerosol were due to different microphysical and chemical properties of the sampled BC.

https://doi.org/10.5194/egusphere-2023-570
Preprint. Discussion started: 11 April 2023

Interestingly almost none of the aerosol were classified as strong BrC and BC/BrC mixture (AAE and SAE values above 1.5), revealing a very low contribution of BrC to the aerosol absorption at PDM. An explanation could be the rapid BrC depletion within the first day after emission, by photobleaching or volatilization that has been observed in several studies (Forrister et al., 2015; Wong et al., 2019; Zeng et al., 2020). Altogether these results suggest that BC were the predominant absorption component of aerosols at PDM and controlled the variation of SSA throughout the two observation years.

https://doi.org/10.5194/egusphere-2023-570
Preprint. Discussion started: 11 April 2023

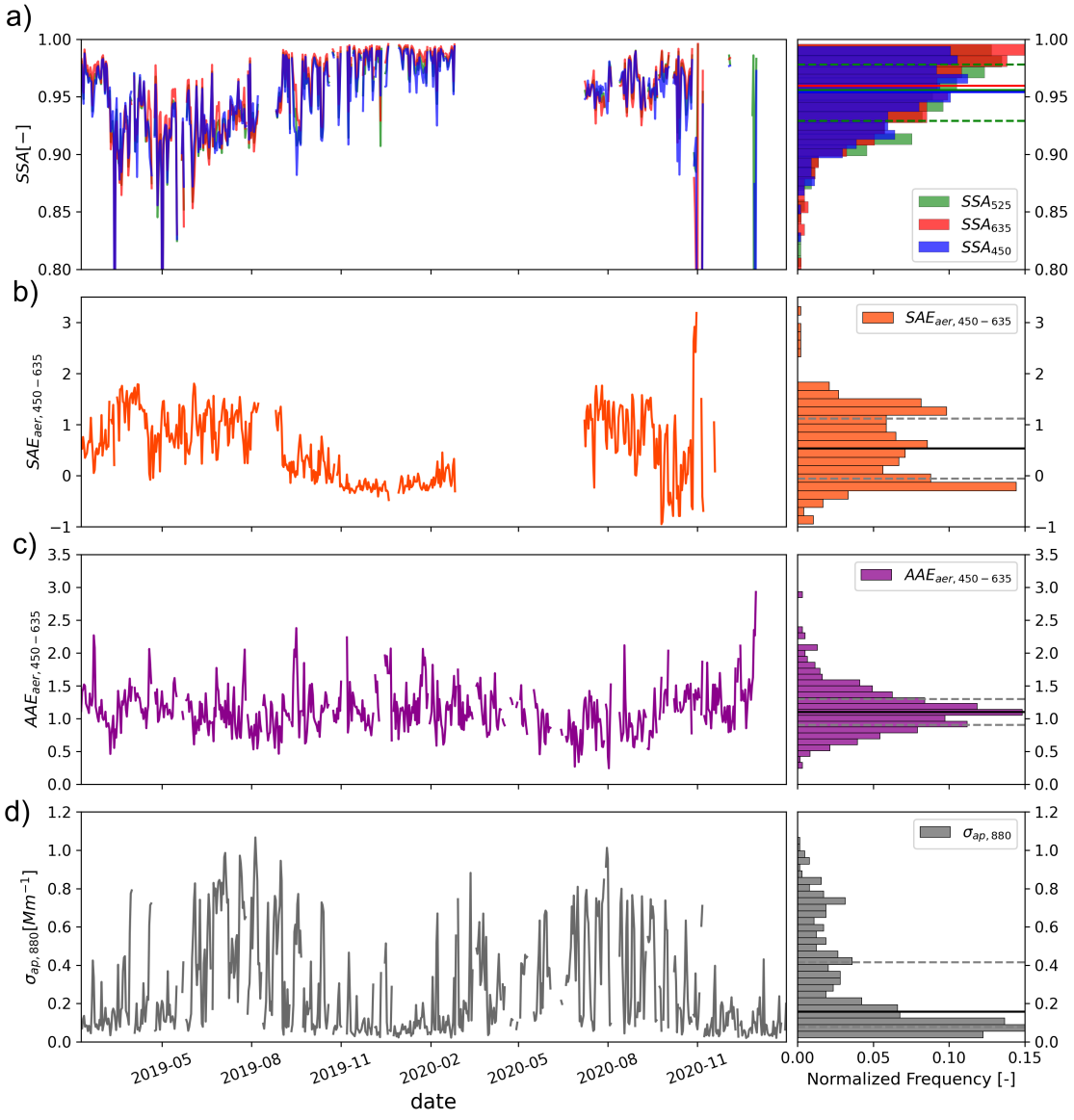

Figure 4. Time series (left) and statistical distributions (median, 25th and 75th percentiles, right) of aerosols optical properties measured at PDM in 2019-2020 with (a) Single Scattering Albedo at 450, 525 and 635 nm, (b) Scattering Angström Exponent at 450-635 nm, (c) Absorption Angström Exponent at 450-635 nm, (d) Absorption coefficient at 880 nm. Daily average data are shown.

https://doi.org/10.5194/egusphere-2023-570
Preprint. Discussion started: 11 April 2023

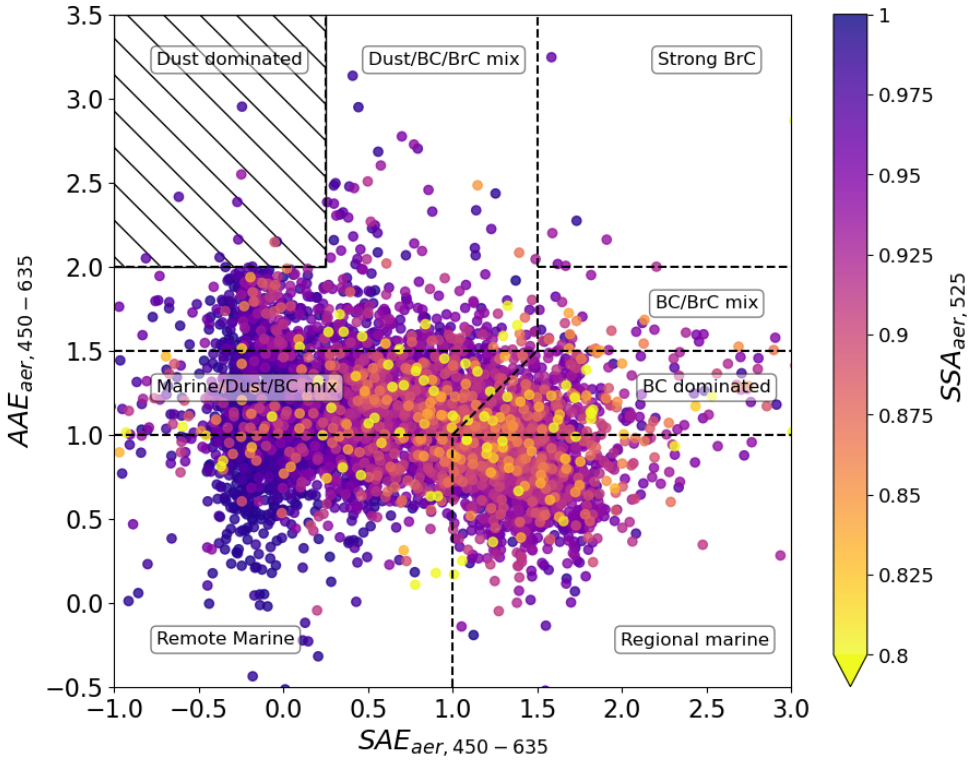

Figure 5. Hourly average Aerosols Absorption Angström Exponent vs. Scattering Angström Exponent calculated at 450-635 nm and colored as a function of the Single Scattering Albedo at 525 nm. The classification of aerosol type by Cappa et al. (2016) is also shown. The points in the dashed zone, representing dust events, were filtered before analyses of BC properties to avoid artifacts in the calculation of MAC_{BC}.

3.3 BC sources and properties

Figure 6 shows the time series of the physical and optical properties of BC. The mean M_{BC}, shown in fig 5a, was 34.8 ± 35.7 (Mean ± STD) ng m^{-3} , which is a typical level for remote mountain sites. For instance, Sun et al. (2021) observed M_{BC}s around 20 ng.m^{-3} from 9-years of measurements with a Multi-Angle Absorption Photometers (MAAP, model 5012, Thermo Scientific) at the Zugspitze-Schneefernerhaus station, Germany (2671 m a.s.l.). Motos et al. (2020)(Motos et al., 2020) measured M_{BC}s around 9 ng m^{-3} in summer at the Jungfraujogh, Switzerland (3580 m a.s.l.). Seasonal variations of M_{BC} (i.e. Fig. 6a) are similar to those of $\sigma_{ap,880}$ (i.e. Fig. 4d) with higher M_{BC} and $\sigma_{ap,880}$ in winter than in summer. BC represented around 7 ± 5 % of the total aerosol number concentration measured by the SMPS over the campaign. An increase of BC number fraction by a factor 2.5 was found in summer (9 ± 5 %) compared to winter (4 ± 3 %). Simultaneously, $\sigma_{ap,880}$ increased by a factor 4 between winter and summer . Thus, it confirms that BC contributed to a significant part of the aerosol absorption at PDM.

https://doi.org/10.5194/egusphere-2023-570
Preprint. Discussion started: 11 April 2023

Bivariate polar plots obtained by combining hourly wind analysis and M_{BC}s are shown in Figure 7 to investigate recent geographical origins of BC in winter and summer. Seasonal differences between the origin of highest M_{BC} are thrown into relief, as well as the footprints of air masses backtrajectory densities plotted in Figure S5 in the Supplement. In summer, the highest M_{BC} was linked to winds from the west and south west, suggesting that regional transport from Atlantic Spain was an important source of BC (Fig 7b). By contrast in winter (Fig 7a), the highest M_{BC} occurred mainly under more static conditions (ie. for wind speeds under 10 m s^{-1}) and BC mostly came from the west and north-east highlighting different BC geographical sources. As a reminder, the locally emitted pollution at the measurement station was filtered before the analysis, limiting local M_{BC} contributions emitted from the PDM station. Further discussion on the role of PBL influence on M_{BC} will be discussed in Section 4.2.

The $\Delta BC/\Delta CO$ emission ratio, presented in Fig. 6b, shows a wide range of values from 0 to 10 ng m^{-3} $ppbv^{-1}$, with a mean value of 1.93 $\pm$ 2.12 ng m^{-3} $ppbv^{-1}$. Summer values were generally higher than winter emission ratios, which could reflect either lower BC scavenging during transport or different emission sources of BC between seasons. Indeed, $\Delta BC/\Delta CO$ emission ratio varies as a function of fuel types, combustion efficiencies and wet deposition by precipitations (Baumgardner et al., 2002; Taylor et al., 2014). This explains the high diversity of $\Delta BC/\Delta CO$ emission ratios obtained in the literature worldwide, going from 0.5 ng m^{-3} $ppbv^{-1}$ at the Jungfraujoch, Switzerland (Liu et al., 2010), to 9 ng m^{-3} $ppbv^{-1}$ in a biomass burning plume above Texas region during TexAQS 2006 campaign, USA (Spackman et al., 2010), if only studies using SP2 measurements are considered. Overall $\Delta BC/\Delta CO$ from fossil fuel tends to exhibit lower values to those from biomass combustion (Guo et al., 2017; Pan et al., 2011; Zhu et al., 2019). To our knowledge the only available $\Delta BC/\Delta CO$ measurement in Europe were performed during airborne measurements in the Cabauw industrial region, Netherlands, by McMeeking et al. (2010), who found very low values around 0.8 ng m^{-3} $ppbv^{-1}$.

BC mass median core size diameter ($D_{BC,core}$) was quite constant during the campaign with a mean geometric diameter of 179 $\pm$ 28 nm (Fig. 6c). An exception occurred in early December 2019, where we detected the presence of large BC particles with $D_{BC,core}$ around 400 nm. However observations during this period may be the results of measurement uncertainties due to too low M_{BC} (less than 10 ng m^{-3}). The $D_{BC,core}$ values obtained at PDM are generally comparable to $D_{BC,core}$ that has been reported to range from 180 to 225 nm for well-aged background BC (Liu et al., 2010; McMeeking et al., 2010; Schwarz et al., 2010; Shiraiwa et al., 2008). However, our values are slightly higher than previous observations at Jungfraujoch by Motos et al. (2020) who reported $D_{BC,core}$ ranging from 130 and 150 nm in summer and winter. Instead of fitting the SP2 observations with a multimodal individual lognormal modes (e.g. Section 2.2.2), Motos et al. (2020) used a single-mode fit diameter approach which may bias the estimated SP2 $D_{BC,core}$ (Tinorua et al., in preparation).

The ambient MAC_{BC} was around 9.8 $\pm$ 2.7 m^2 g^{-1} at 880 nm (Figure 6d) with systematically higher values in summer . This stands in the highest part of the range from 5.3 to 9.5 m^2 g^{-1} previously reported for measurements at European mountain stations by Pandolfi et al. (2014),Yus-Díez et al. (2022) and Zanatta et al. (2016). However these studies used different measurement techniques and corrections factors for estimating MAC_{BC} that causes significant uncertainty. Because of the absence of a standard method for quantifying M_{BC}, the absolute uncertainties on the literature MAC values are very

https://doi.org/10.5194/egusphere-2023-570
Preprint. Discussion started: 11 April 2023

high ranging from ±30 to 70%, making difficult the comparison of MAC_{BC} derived from different instruments (Zanatta et al., 2016).

Variations in MAC_{BC} may exist for different reasons. We first addressed the question of whether the MAC_{BC} depends on $D_{BC,core}$ in Figure S6 in the Supplement. There was no clear correlation between MAC_{BC} and $D_{BC,core}$, which indicates that the variation in BC size was not the cause of the MAC_{BC} variability. This is because $D_{BC,core}$ only varied within a relatively narrow range (percentiles 25 and 75 around 164 and 195 nm) during the campaign. The observed MAC_{BC} values were converted to equivalent E_{abs}, by dividing them by a reference MAC for pure uncoated BC ($MAC_{bare,BC}$). While values of $MAC_{bare,BC}$ are reported in the literature, estimation of campaign-specific $MAC_{bare,BC}$ allows for more robust determination of E_{abs} than using values from the literature since $MAC_{bare,BC}$ is dependent of the size of uncoated BC (Bond and Bergstrom, 2006; Adachi et al., 2007, 2010; Adachi and Buseck, 2013; Cappa et al., 2012). Here $MAC_{bare,BC}$ had an average value of 4.15 $m^2\ g^{-1}$ with values ranging from 3.90 to 4.37 $m^2\ g^{-1}$ considering the standard deviation of the mean $D_{BC,core}$, which is in reasonable agreement with literature assessments (Liu et al., 2020b).

https://doi.org/10.5194/egusphere-2023-570
Preprint. Discussion started: 11 April 2023

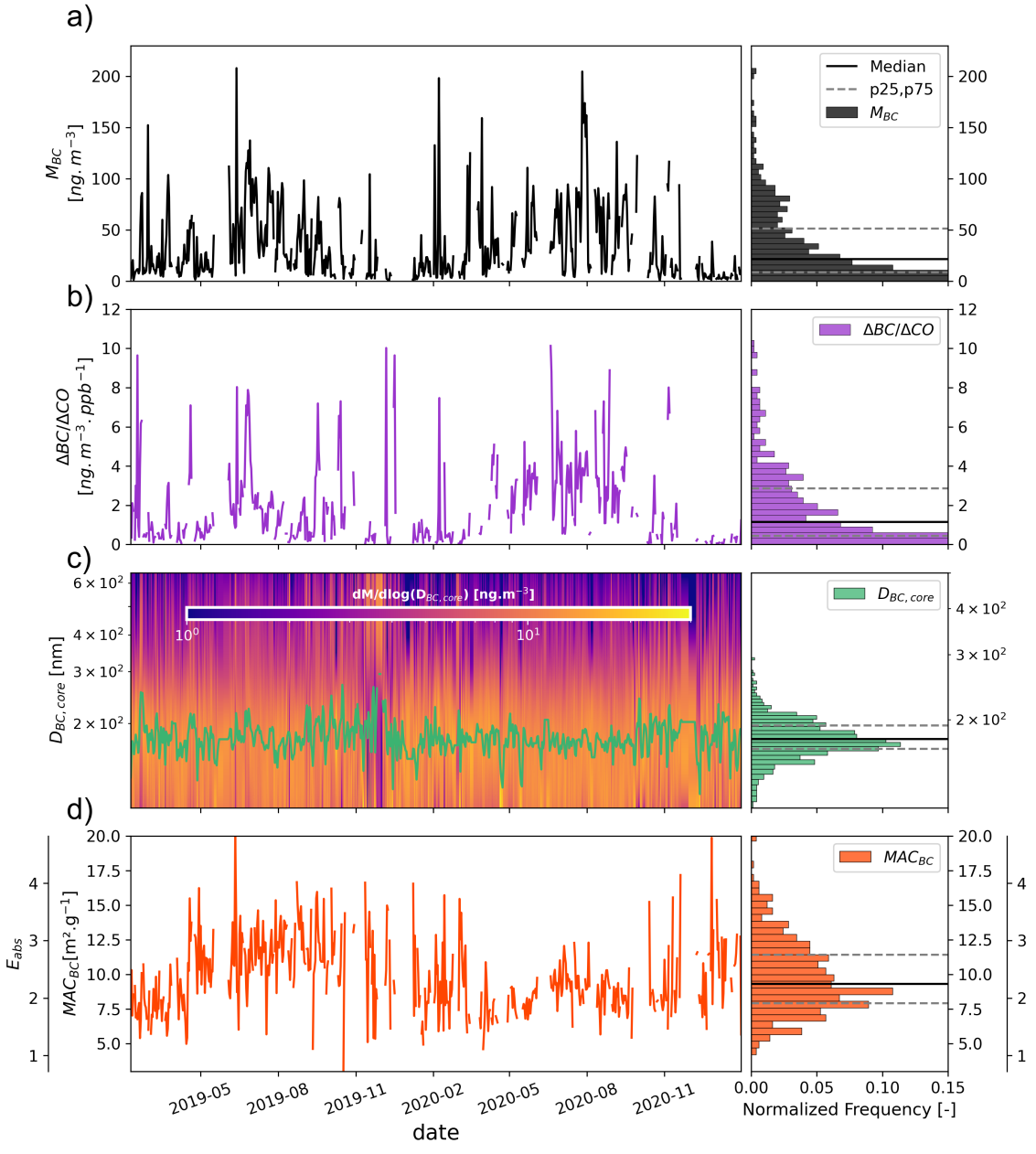

Figure 6. Time series (left) and statistical distributions (median, 25th and 75th percentiles, right) of BC properties measured at PDM in 2019-2020. (a) BC mass concentration, (b) ΔBC/ΔCO emission ratio, (c) BC core mass size distribution with geometric diameter on green solid line, (d) BC Mass Absorption Cross-Section and Absorption Enhancement at 880 nm. Daily average data are shown.

https://doi.org/10.5194/egusphere-2023-570
Preprint. Discussion started: 11 April 2023

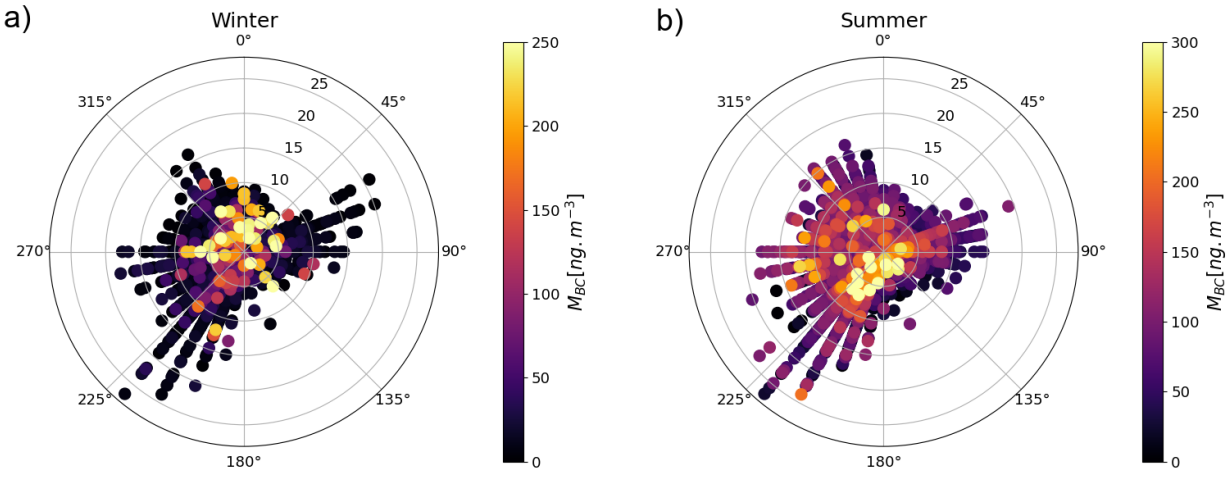

Figure 7. Bivariate polar plots of hourly mean BC concentration measured by the SP2 as a function of wind direction and speed in a) winter and b) summer.

The E_{abs} values derived from MAC_{BC} observations were significantly greater than unity with mean value of 2.4 ±0.7 (Figure 6d). Given the remote mountain location and presumable distance from fresh BC sources, it is expected that the BC particles reaching PDM would be aged and relatively thickly coated. The most likely reason for the strong E_{abs} is a lensing effect due to the internal mixing of BC with other particles that drives MAC_{BC} variability, though we cannot eliminate changes in BC morphology that can result from coating onto BC. There was a significant seasonal trend in E_{abs} with higher values observed in summer, indicating that BC reaching the PDM station has undergone longer aging processes during this season. These results are consistent with the measurements of Motos et al. (2020) at the Jungfraujoch, which also indicated a strong seasonality in BC mixing state with larger coating in summer. Figure 8 further shows the diurnal variation of E_{abs} for every seasons. There was a remarkable opposite diurnal profile between seasons in E_{abs} with midday showing a minimum around 1.7 in winter, and a maximum around 2.9 in summer. Spring and autumn showed intermediate patterns with less regular E_{abs} throughout the day. These observations suggest that different sources and/or processes drove the seasonal contrast in BC properties. The following section aims at investigating potential drivers of E_{abs} variations, including BC wet scavenging, dominant BC sources and transport pathways.

https://doi.org/10.5194/egusphere-2023-570
Preprint. Discussion started: 11 April 2023

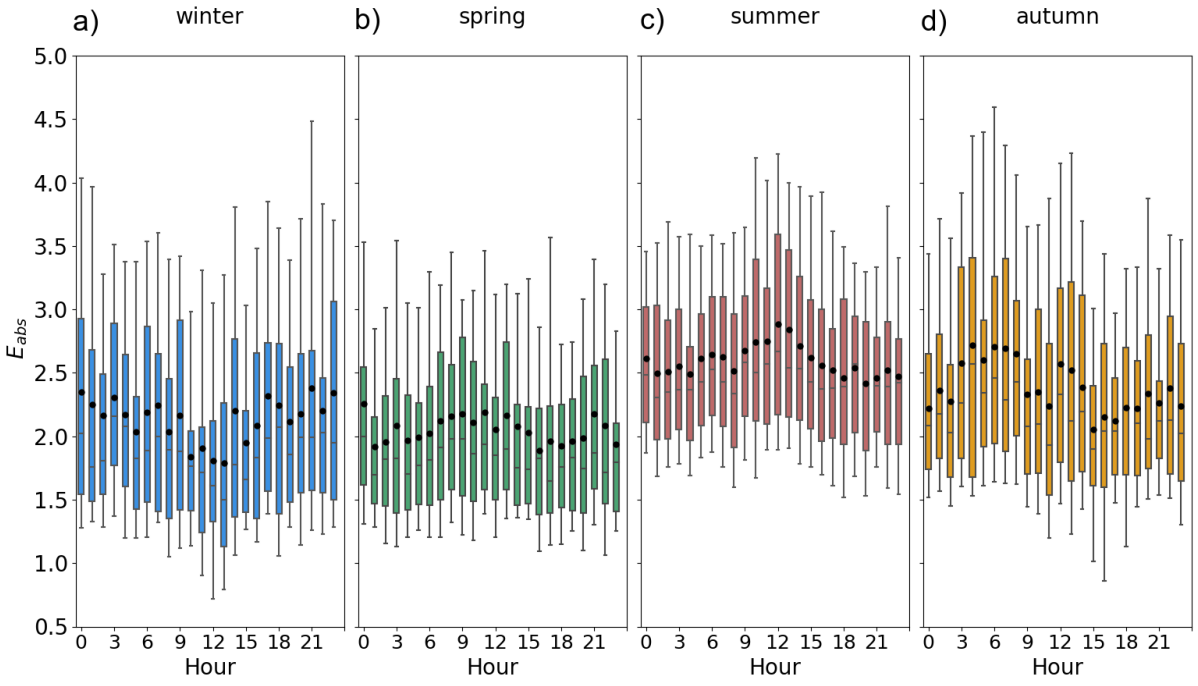

Figure 8. Diurnal cycles of E_{abs} for each season during 2019-2020 period. Winter includes December, January and February, spring covers March April and May, summer includes June, July and August and months from September to November are grouped together in autumn. Boxes, lines, black dots and whiskers indicate 25th percentile, 75th percentile, median, mean, 10th percentile and 90th percentile, respectively.

4 Investigation of factors influencing BC properties

4.1 The impact of BC wet scavenging on BC properties

We first investigated whether E_{abs} was modulated by a size-dependent BC wet scavenging process during precipitation along their transport pathway. This hypothesis is based on the fact that the removal of particles is favored for the largest and thickly coated BC because the activation of aerosols to cloud droplets is predominantly controlled by the particle size (Moteki et al., 2012; Motos et al., 2019; Ohata et al., 2016; Zhang et al., 2021). The wet removal of BC was investigated by performing a cluster analysis using $\Delta BC/\Delta CO$ data for which precipitation occurred or not along 72h back trajectories computed by the HYSPLIT model. Figure 9a shows significantly lower $\Delta BC/\Delta CO$ for air masses affected by precipitations. The reduction of $\Delta BC/\Delta CO$ by $\sim$ 40 % suggests that a significant removal process of BC from the precipitation occurred long the transport pathway. This result is confirmed by the dependence of $\Delta BC/\Delta CO$ to RH in Figure 9b, where a sudden decline of $\Delta BC/\Delta CO$ appeared for highest RH>80%. Figures 9 c-d show in contrast little influence of precipitation and RH on E_{abs}. Furthermore, the resultant BC after precipitations exhibited similar core size, as shown in Fig. S7 in the Supplement. Therefore we conclude that BC wet scavenging did not significantly affect the size of BC-containing particles to drive changes in E_{abs}.

https://doi.org/10.5194/egusphere-2023-570
Preprint. Discussion started: 11 April 2023

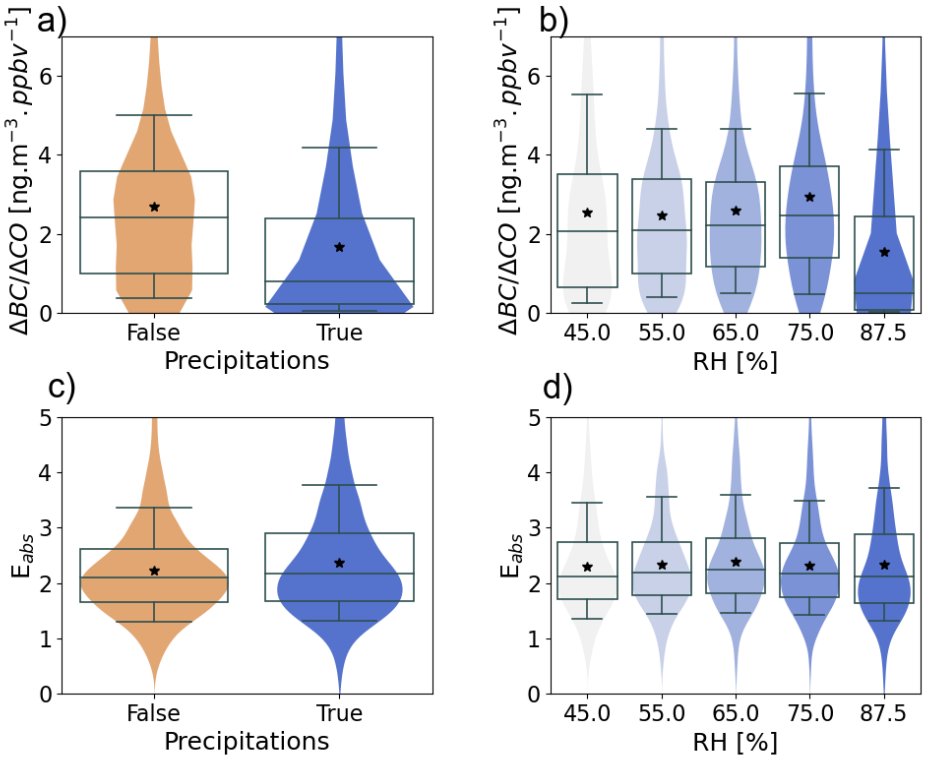

Figure 9. ΔBC/ΔCO emission ratio and E_{abs} vs. a) and c) precipitations along the air mass back trajectory calculated with HYSPLIT model and b) and d) Relative Humidity measured at PDM. Violin plots represent the probability density function of each parameter. Statistics of the boxplots are the same as Fig. 7.

This result contradicts with previous studies showing a decrease in BC size due to wet scavenging (Kondo et al., 2016; Moteki et al., 2012; Taylor et al., 2014; Liu et al., 2020a). It could be explained by the size of BC core sampled at PDM that was higher than the one described in these studies. Hoyle et al. (2016) evidenced at the Junfraujoch a threshold diameter of around 90 nm above which a particle activates to a droplet upon cloud formation. The majority of BC sampled at PDM exhibited $D_{BC,core}$ above this critical diameter. Droplet activation of an aerosol particle occurs when the supersaturation of the surrounding water vapor exceeds a critical value of supersaturation. As the ambient supersaturation varies depending on the environment, it is difficult to conclude whether the insensitivity of BC size distribution and E_{abs} to precipitation occurrence during the 72-h air mass history was solely due to the presence of large BC particles or to a high ambient supersaturation. Further measurements of simultaneous BC wet removal and effective supersaturation are needed to test these assumptions.

https://doi.org/10.5194/egusphere-2023-570
Preprint. Discussion started: 11 April 2023

4.2 The contrasted seasonal influence of FT and PBL on BC properties

Figure 10 shows the BC properties classified by FT- and PBL-conditions (methodology in Section 2.5) and by seasons. Air masses for which precipitation occurred along 72-h back trajectories computed by the HYSPLIT model where removed for this analysis.

In winter 75 % of the M_{BC} values were found under 105 ng m^{-3} under PBL-influence, whereas under FT conditions they were under 45 ng m^{-3} (Figure 10a). Furthermore the diurnal cycle of M_{BC} in winter PBL-influenced conditions showed enhancement in the daytime (Figure S8 in Supplement). This trend is consistent with intrusions of pollutants transported from PBL sources through convective mixing. During the night, the nocturnal depressed PBL in the valleys and the plain trapped the surface pollution below the mountain summits, and the subsiding cleaner air in the FT may have diluted the BC quantity at PDM. The higher $\Delta BC/\Delta CO$ in PBL-conditions than FT-conditions may indicate additional sources from biomass combustion (Fig 10c), which could be attributed to either residential wood heating or stubble-burning that is still a common practice in the Pyrenees (González-Olabarria et al., 2015). Figure 10b shows that E_{abs} was modulated by the atmospheric dynamic in winter with lower values in PBL-influenced conditions than FT-influenced conditions. Therefore the significant decrease of E_{abs} observed at noon in winter (Figure 8a) might be the result of BC particles directly uplifted from the PBL, which have undergone shorter aging processes and less coating than BC transported into the FT.

During summer vertical transport from the PBL occurred about half of the days analyzed in this study. Surprisingly these thermally driven PBL injection did not significantly impact M_{BC} (Figure 10d). This contrasts with our winter observations and most previous surface measurements at mountain sites, where the daytime PBL development had been shown to enhance aerosol mass concentration (Herrmann et al., 2015; Venzac et al., 2009). $\Delta BC/\Delta CO$ in BL- and FT-conditions were close to each other, with values around 2.8 $\pm$ 1.6 ng m^{-3}.$ppbv^{-1}$ (Mean $\pm$ STD) and 3.3 $\pm$ 1.7 ng.m^{-3} $ppbv^{-1}$, respectively (Figure 10f), suggesting that the FT has a significant background load in BC at the continental scale, which limits the relative influence of PBL injection on M_{BC} during summer. The resulting E_{abs} was remarkably similar for PBL vs. FT air mass categories (Figure 10e). This is an evidence that the background FT may be greatly influenced by biomass burning in Europe. For example (Petetin et al., 2018) have shown that biomass burning aerosol accounts for about 43 - 81% of the CO concentration in lower FT in summer using in situ airborne observations of CO from the IAGOS program. The ubiquitous presence of dilute biomass burning in the FT and its significant contribution to aerosol mass loading was also established using airborne measurements of ozone and precursor source tracers from the NASA Atmospheric Tomography mission (Bourgeois et al., 2021; Schill et al., 2020). These findings are consistent with the higher $\Delta BC/\Delta CO$ observed in the summertime at PDM, indicating potential additional sources from biomass burning. Given that the majority of trajectories reaching PDM in summer traveled over the Iberian Peninsula (Fig. S5 in the Supplement), and prior to this, as far as North Africa and the North America where large fire events frequently occur, it is a possible explanation for stable concentrations of highly absorbing BC observed at PDM during summer. Additional measurements of the aerosol chemical composition and a precise source apportionment should be performed to confirm this.

https://doi.org/10.5194/egusphere-2023-570
Preprint. Discussion started: 11 April 2023

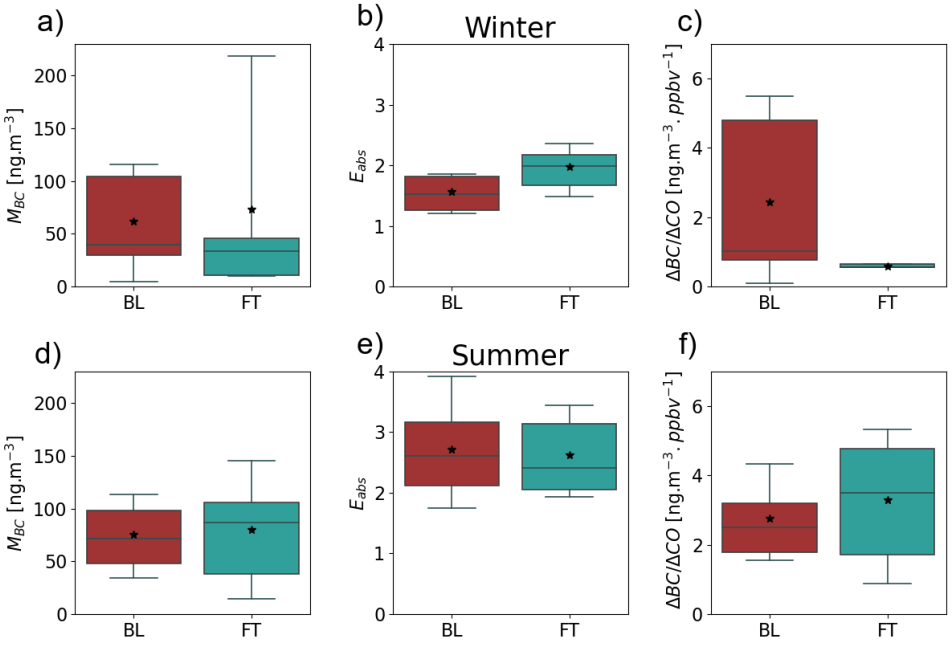

Figure 10. (a) BC mass concentrations, (b) MAC_{BC} and (c) $\Delta BC/\Delta CO$ emission ratio as a function of the predominant influence at PDM in winter. The same for summer are given in d), e) and f). Red boxplots represents Boundary Layer conditions and green boxes are Free Tropospheric conditions. Precipitation events were filtered before analyses.

A question remains about the cause of the diurnal variation of E_{abs} in summer (Figure 8c). As shown in Figure S9, the E_{abs} increase was not temporally correlated with the wind direction change from West-South-West to South, as evidenced by the 2-h delay between the two events. Furthermore, while the E_{abs} increase occurs when $\Delta BC/\Delta CO$ decreases, the E_{abs} drop in the afternoon was not accompanied by an increase in $\Delta BC/\Delta CO$. Then increase of E_{abs} in the morning was most likely due to further aging and becoming heavily coated BC rather than a change in BC emission source. Several studies highlighted the major role of photochemical processing and extensive secondary aerosol generation to promote the light absorption enhancement of BC (Knox et al., 2009; Krasowsky et al., 2016; Liu et al., 2019; Wang et al., 2017; Xu et al., 2018; Yus-Díez et al., 2022). At PDM the enhanced E_{abs} at noon was accompanied by a strong elevation of particle number concentration in the diameter range 10-30 nm and a shift of the aerosol accumulation mode towards larger sizes, thus revealing both new particle formation and condensation onto preexisting particles (Figure S10 in the Supplement). This evidence imply the potential role of photochemical processing on BC in regulating the diurnal dynamics of E_{abs}.

5 Conclusions

Continuous two-year measurements of BC properties and additional aerosol characteristics have been performed at the high-altitude mountain site Pic du Midi in the French Pyrenees. The classification of the dominant aerosol type using the spectral

https://doi.org/10.5194/egusphere-2023-570
Preprint. Discussion started: 11 April 2023

aerosol optical properties indicates that BC is the predominant absorption component of aerosols at PDM and controls the variation of SSA throughout the two years. The lower SSA in summer (0.93) than winter (0.97) is correlated with a higher BC number fraction. AAE values around 1.13 ± 0.35 indicates a negligible influence of BrC to the aerosol absorption properties. SSA for dust-dominated aerosol were quite similar as those for remote marine aerosol, indicating that dust particles were not absorbing enough to substantially lower the aerosol SSA at PDM.

MAC strongly regulates BC radiative forcing, heating effect and interactions with snow. It is not clear if BC at high-altitude mountain sites should have a thicker or thinner coating than in urban or plain sites or even should be coated at all. On the one hand, the longer BC lifetime and the low temperature in the FT favor thicker coating due to enhanced condensation of low-volatility compounds in colder environment. On the other hand, the low concentrations of particles and gaseous precursors in the FT may limit the coating processes. Our two-year long observations show that the overall net effect is a strong absorption enhancement with a mean E_{abs} value of 2.4 ± 0.7.

A significant reduction of $\Delta BC/\Delta CO$ when precipitation occurred along the air mass transport suggests wet removal of BC. However the wet removal process has been found not to affect the size of BC-containing particles, resulting in unchanged E_{abs}. This contrasts with previous observations showing a preferential removal of BC with large sizes (Kondo et al., 2016; Moteki et al., 2012; Taylor et al., 2014; Liu et al., 2020a). The difference may be due to either larger BC particles sampled at PDM ($D_{BC,core}$ around 180 nm) or different meteorological conditions such as ambient supersaturation in precipitating clouds.

In addition, a large seasonal contrast in BC properties has been discovered, with higher M_{BC} and E_{abs} in summer than winter. In winter a strong diurnal variability of M_{BC} (E_{abs}) with higher (lower) values in the middle of the day was linked to the injection of BC originating from the PBL into a clean free troposphere. Many rural regions in the Pyrenees rely on wood burning for home heating during this season that may provide a significant source of BC at PDM. By contrast, during summer, the diurnal variation of M_{BC} was rather constant despite more frequent PBL-conditions, implying that M_{BC} fluctuations were rather dominated by regional and long-range transport in the FT. Evidence suggests that biomass burning emissions from fires effectively altered the concentration and optical properties of BC at PDM, leading to higher E_{abs} in summer compared to winter. The diurnal cycle of E_{abs} was opposite to that in winter with maximum values of ~ 2.9 observed at noon. We suggest that this daily variation results from photochemical processing driving BC mixing state rather than a change in BC emission source. Additional measurements of the chemical composition in both the gas- and particle-phases are required to confirm this.

All these results on BC properties and notably their consequences on aerosol absorption are essential to better understand the role of BC in the climate system. In the light of the results obtained in the present study, BC absorption might not be correctly represented in many climate models. In particular, wet removal is an important process for climate modeling by moderating BC number and mass concentrations, lifetime and vertical distributions. Results here show that this wet removal of BC should be independent of the BC size and its mixing state, implying that the hydrophilic/hydrophobic separation that could be done in some models may not be appropriate. Besides, our results also tend to show that it would be difficult for a climate model to correctly represent the MAC_{BC} and its variations without properly taking into account the diversity of sources and the different processes leading to its aging during transport.

https://doi.org/10.5194/egusphere-2023-570
Preprint. Discussion started: 11 April 2023

Data availability. Aerosol microphysical and optical properties are freely available at http://ebas.nilu.no/ (NILU, 2018). CO data are available on the ICOS platform at https://www.icos-cp.eu/. BC data are available upon request to the authors.

Author contributions. CD and ST designed the study, developed the analysis protocols, and wrote the initial manuscript. PN contributed to the data analysis. FG and VP provided data and methods to analyse them. TB, FG, EL, ST, VP and CD contributed to the measurement campaign. All authors reviewed the final manuscript.

Competing interests. The authors declare that they have no conflict of interest.

Acknowledgements. This work received funding from the French national program LEFE/INSU and Météo-France. Observation data were collected at the Pyrenean Platform for Observation of the Atmosphere P2OA (http://p2oa.aero.obs-mip.fr). P2OA facilities and staff are funded and supported by the University Paul Sabatier Toulouse 3, France, and CNRS (Centre National de la Recherche Scientifique). We especially thank the staff of the Pic du Midi platform (Observatoire Midi-Pyrénées) for their technical assistance. We acknowledge the SNO ICOS-France and ACTRIS-France forsupporting greenhouse gases and aerosol observations at PDM, data collection, processing and dissemination. We also acknowledge the use of the HYSPLIT model and READY websitefrom the NOAA Air Ressources Laboratory (http://ready.arl.noaa.gov).

https://doi.org/10.5194/egusphere-2023-570
Preprint. Discussion started: 11 April 2023

References

Adachi, K. and Buseck, P. R.: Changes of ns-soot mixing states and shapes in an urban area during CalNex, Journal of Geophysical Research: Atmospheres, 118, 3723–3730, https://doi.org/10.1002/jgrd.50321, _eprint: https://agupubs.onlinelibrary.wiley.com/doi/pdf/10.1002/jgrd.50321, 2013.

Adachi, K., Chung, S. H., Friedrich, H., and Buseck, P. R.: Fractal parameters of individual soot particles determined using electron tomography: Implications for optical properties, Journal of Geophysical Research: Atmospheres, 112, https://doi.org/10.1029/2006JD008296, _eprint: https://onlinelibrary.wiley.com/doi/pdf/10.1029/2006JD008296, 2007.

Adachi, K., Chung, S. H., and Buseck, P. R.: Shapes of soot aerosol particles and implications for their effects on climate, Journal of Geophysical Research: Atmospheres, 115, https://doi.org/10.1029/2009JD012868, _eprint: https://agupubs.onlinelibrary.wiley.com/doi/pdf/10.1029/2009JD012868, 2010.

Andrews, E., Ogren, J. A., Bonasoni, P., Marinoni, A., Cuevas, E., Rodríguez, S., Sun, J. Y., Jaffe, D. A., Fischer, E. V., Baltensperger, U., Weingartner, E., Coen, M. C., Sharma, S., Macdonald, A. M., Leaitch, W. R., Lin, N. H., Laj, P., Arsov, T., Kalapov, I., Jefferson, A., and Sheridan, P.: Climatology of aerosol radiative properties in the free troposphere, Atmospheric Research, 102, 365–393, https://doi.org/10.1016/j.atmosres.2011.08.017, 2011.

Baumgardner, D., Raga, G., Peralta, O., Rosas, I., Castro, T., Kuhlbusch, T., John, A., and Petzold, A.: Diagnosing black carbon trends in large urban areas using carbon monoxide measurements, Journal of Geophysical Research: Atmospheres, 107, ICC 4–1–ICC 4–9, https://doi.org/10.1029/2001JD000626, _eprint: https://onlinelibrary.wiley.com/doi/pdf/10.1029/2001JD000626, 2002.

Beeler, P. and Chakrabarty, R. K.: Constraining the particle-scale diversity of black carbon light absorption using a unified framework, Atmospheric Chemistry and Physics, 22, 14 825–14 836, https://doi.org/10.5194/acp-22-14825-2022, publisher: Copernicus GmbH, 2022.

Bellouin, N., Quaas, J., Gryspeerdt, E., Kinne, S., Stier, P., Watson-Parris, D., Boucher, O., Carslaw, K. S., Christensen, M., Daniau, A.-L., Dufresne, J.-L., Feingold, G., Fiedler, S., Forster, P., Gettelman, A., Haywood, J. M., Lohmann, U., Malavelle, F., Mauritsen, T., McCoy, D. T., Myhre, G., Mülmenstädt, J., Neubauer, D., Possner, A., Rugenstein, M., Sato, Y., Schulz, M., Schwartz, S. E., Sourdeval, O., Storelvmo, T., Toll, V., Winker, D., and Stevens, B.: Bounding Global Aerosol Radiative Forcing of Climate Change, Reviews of Geophysics, 58, e2019RG000 660, https://doi.org/10.1029/2019RG000660, _eprint: https://agupubs.onlinelibrary.wiley.com/doi/pdf/10.1029/2019RG000660, 2020.

Bond, T. and Bergstrom: Light Absorption by Carbonaceous Particles: An Investigative Review, Aerosol Sci. Tecnol., 40, 27–67, https://doi.org/10.1080/02786820500421521, 2006.

Bond, T. C., Doherty, S. J., Fahey, D. W., Forster, P. M., Berntsen, T., DeAngelo, B. J., Flanner, M. G., Ghan, S., Kärcher, B., Koch, D., Kinne, S., Kondo, Y., Quinn, P. K., Sarofim, M. C., Schultz, M. G., Schulz, M., Venkataraman, C., Zhang, H., Zhang, S., Bellouin, N., Guttikunda, S. K., Hopke, P. K., Jacobson, M. Z., Kaiser, J. W., Klimont, Z., Lohmann, U., Schwarz, J. P., Shindell, D., Storelvmo, T., Warren, S. G., and Zender, C. S.: Bounding the role of black carbon in the climate system: A scientific assessment, Journal of Geophysical Research: Atmospheres, 118, 5380–5552, https://doi.org/https://doi.org/10.1002/jgrd.50171, _eprint: https://agupubs.onlinelibrary.wiley.com/doi/pdf/10.1002/jgrd.50171, 2013.

Boucher, O., Balkanski, Y., Hodnebrog, , Myhre, C. L., Myhre, G., Quaas, J., Samset, B. H., Schutgens, N., Stier, P., and Wang, R.: Jury is still out on the radiative forcing by black carbon, Proceedings of the National Academy of Sciences, 113, E5092–E5093, https://doi.org/10.1073/pnas.1607005113, publisher: Proceedings of the National Academy of Sciences, 2016.

https://doi.org/10.5194/egusphere-2023-570
Preprint. Discussion started: 11 April 2023

Bourgeois, I., Peischl, J., Neuman, J. A., Brown, S. S., Thompson, C. R., Aikin, K. C., Allen, H. M., Angot, H., Apel, E. C., Baublitz, C. B., Brewer, J. F., Campuzano-Jost, P., Commane, R., Crounse, J. D., Daube, B. C., DiGangi, J. P., Diskin, G. S., Emmons, L. K., Fiore, A. M., Gkatzelis, G. I., Hills, A., Hornbrook, R. S., Huey, L. G., Jimenez, J. L., Kim, M., Lacey, F., McKain, K., Murray, L. T., Nault, B. A., Parrish, D. D., Ray, E., Sweeney, C., Tanner, D., Wofsy, S. C., and Ryerson, T. B.: Large contribution of biomass burning emissions to ozone throughout the global remote troposphere, Proceedings of the National Academy of Sciences, 118, e2109628 118, https://doi.org/10.1073/pnas.2109628118, publisher: Proceedings of the National Academy of Sciences, 2021.

Bukowiecki, N., Weingartner, E., Gysel, M., Coen, M. C., Zieger, P., Herrmann, E., Steinbacher, M., Ga¨ggeler, H. W., and Baltensperger, U.: A Review of More than 20 Years of Aerosol Observation at the High Altitude Research Station Jungfraujoch, Switzerland (3580 m asl), Aerosol and Air Quality Research, 16, 764–788, https://doi.org/10.4209/aaqr.2015.05.0305, publisher: Taiwan Association for Aerosol Research, 2016.

Cappa, C. D., Onasch, T. B., Massoli, P., Worsnop, D. R., Bates, T. S., Cross, E. S., Davidovits, P., Hakala, J., Hayden, K. L., Jobson, B. T., Kolesar, K. R., Lack, D. A., Lerner, B. M., Li, S.-M., Mellon, D., Nuaaman, I., Olfert, J. S., Petäjä, T., Quinn, P. K., Song, C., Subramanian, R., Williams, E. J., and Zaveri, R. A.: Radiative Absorption Enhancements Due to the Mixing State of Atmospheric Black Carbon, Science, 337, 1078–1081, https://doi.org/10.1126/science.1223447, publisher: American Association for the Advancement of Science, 2012.

Cappa, C. D., Kolesar, K. R., Zhang, X., Atkinson, D. B., Pekour, M. S., Zaveri, R. A., Zelenyuk, A., and Zhang, Q.: Understanding the optical properties of ambient sub- and supermicron particulate matter: results from the CARES 2010 field study in northern California, Atmospheric Chemistry and Physics, 16, 6511–6535, https://doi.org/10.5194/acp-16-6511-2016, publisher: Copernicus GmbH, 2016.

Chambers, S. D., Zahorowski, W., Williams, A. G., Crawford, J., and Griffiths, A. D.: Identifying tropospheric baseline air masses at Mauna Loa Observatory between 2004 and 2010 using Radon-222 and back trajectories, Journal of Geophysical Research: Atmospheres, 118, 992–1004, https://doi.org/10.1029/2012JD018212, _eprint: https://agupubs.onlinelibrary.wiley.com/doi/pdf/10.1029/2012JD018212, 2013.

China, S., Mazzoleni, C., Gorkowski, K., Aiken, A. C., and Dubey, M. K.: Morphology and mixing state of individual freshly emitted wildfire carbonaceous particles, Nat Commun, 4, 2122, https://doi.org/10.1038/ncomms3122, number: 1 Publisher: Nature Publishing Group, 2013.

Collaud Coen, M., Weingartner, E., Furger, M., Nyeki, S., Prévôt, A. S. H., Steinbacher, M., and Baltensperger, U.: Aerosol climatology and planetary boundary influence at the Jungfraujoch analyzed by synoptic weather types, Atmospheric Chemistry and Physics, 11, 5931–5944, https://doi.org/10.5194/acp-11-5931-2011, publisher: Copernicus GmbH, 2011.

Collaud Coen, M., Andrews, E., Aliaga, D., Andrade, M., Angelov, H., Bukowiecki, N., Ealo, M., Fialho, P., Flentje, H., Hallar, A. G., Hooda, R., Kalapov, I., Krejci, R., Lin, N.-H., Marinoni, A., Ming, J., Nguyen, N. A., Pandolfi, M., Pont, V., Ries, L., Rodríguez, S., Schauer, G., Sellegri, K., Sharma, S., Sun, J., Tunved, P., Velasquez, P., and Ruffieux, D.: Identification of topographic features influencing aerosol observations at high altitude stations, Atmospheric Chemistry and Physics, 18, 12 289–12 313, https://doi.org/10.5194/acp-18-12289-2018, publisher: Copernicus GmbH, 2018.

Denjean, C., Formenti, P., Desboeufs, K., Chevaillier, S., Triquet, S., Maillé, M., Cazaunau, M., Laurent, B., Mayol-Bracero, O. L., Vallejo, P., Quiñones, M., Gutierrez-Molina, I. E., Cassola, F., Prati, P., Andrews, E., and Ogren, J.: Size distribution and optical properties of African mineral dust after intercontinental transport, Journal of Geophysical Research: Atmospheres, 121, 7117–7138, https://doi.org/10.1002/2016JD024783, _eprint: https://agupubs.onlinelibrary.wiley.com/doi/pdf/10.1002/2016JD024783, 2016.

https://doi.org/10.5194/egusphere-2023-570
Preprint. Discussion started: 11 April 2023

Denjean, C., Brito, J., Libois, Q., Mallet, M., Bourrianne, T., Burnet, F., Dupuy, R., Flamant, C., and Knippertz, P.: Unexpected Biomass Burning Aerosol Absorption Enhancement Explained by Black Carbon Mixing State, Geophysical Research Letters, 47, e2020GL089 055, https://doi.org/10.1029/2020GL089055, publisher: John Wiley & Sons, Ltd, 2020.

Draxler, R. R. and Hess, G. D.: Description of the HYSPLIT_4 modeling system. NOAA Tech. Memo. ERL ARL-224, 24, 1997.

Drinovec, L., Močnik, G., Zotter, P., Prévôt, A. S. H., Ruckstuhl, C., Coz, E., Rupakheti, M., Sciare, J., Müller, T., Wiedensohler, A., and Hansen, A. D. A.: The "dual-spot" Aethalometer: an improved measurement of aerosol black carbon with real-time loading compensation, Atmospheric Measurement Techniques, 8, 1965–1979, https://doi.org/10.5194/amt-8-1965-2015, publisher: Copernicus GmbH, 2015.

Dumont, M., Gascoin, S., Réveillet, M., Voisin, D., Tuzet, F., Arnaud, L., Bonnefoy, M., Bacardit Peñarroya, M., Carmagnola, C., Deguine, A., Diacre, A., Dürr, L., Evrard, O., Fontaine, F., Frankl, A., Fructus, M., Gandois, L., Gouttevin, I., Gherab, A., Hagenmuller, P., Hansson, S., Herbin, H., Josse, B., Jourdain, B., Lefevre, I., Le Roux, G., Libois, Q., Liger, L., Morin, S., Petitprez, D., Robledano, A., Schneebeli, M., Salze, P., Six, D., Thibert, E., Trachsel, J., Vernay, M., Viallon-Galinier, L., and Voiron, C.: Spatial variability of Saharan dust deposition revealed through a citizen science campaign, Earth System Science Data Discussions, pp. 1–31, https://doi.org/10.5194/essd-2023-16, publisher: Copernicus GmbH, 2023.

Fierce, L., Onasch, T. B., Cappa, C. D., Mazzoleni, C., China, S., Bhandari, J., Davidovits, P., Fischer, D. A., Helgestad, T., Lambe, A. T., Sedlacek, A. J., Smith, G. D., and Wolff, L.: Radiative absorption enhancements by black carbon controlled by particle-to-particle heterogeneity in composition, Proceedings of the National Academy of Sciences, 117, 5196–5203, https://doi.org/10.1073/pnas.1919723117, publisher: Proceedings of the National Academy of Sciences, 2020.

Forrister, H., Liu, J., Scheuer, E., Dibb, J., Ziemba, L., Thornhill, K. L., Anderson, B., Diskin, G., Perring, A. E., Schwarz, J. P., Campuzano-Jost, P., Day, D. A., Palm, B. B., Jimenez, J. L., Nenes, A., and Weber, R. J.: Evolution of brown carbon in wildfire plumes, Geophysical Research Letters, 42, 4623–4630, https://doi.org/10.1002/2015GL063897, _eprint: https://agupubs.onlinelibrary.wiley.com/doi/pdf/10.1002/2015GL063897, 2015.

Fu, X., Marusczak, N., Heimbürger, L.-E., Sauvage, B., Gheusi, F., Prestbo, E. M., and Sonke, J. E.: Atmospheric mercury speciation dynamics at the high-altitude Pic du Midi Observatory, southern France, Atmospheric Chemistry and Physics, 16, 5623–5639, https://doi.org/10.5194/acp-16-5623-2016, publisher: Copernicus GmbH, 2016.

Gao, R. S., Schwarz, J. P., Kelly, K. K., Fahey, D. W., Watts, L. A., Thompson, T. L., Spackman, J. R., Slowik, J. G., Cross, E. S., Han, J.-H., Davidovits, P., Onasch, T. B., and Worsnop, D. R.: A Novel Method for Estimating Light-Scattering Properties of Soot Aerosols Using a Modified Single-Particle Soot Photometer, null, 41, 125–135, https://doi.org/10.1080/02786820601118398, publisher: Taylor & Francis, 2007.

Gao, Y., Chen, F., Lettenmaier, D. P., Xu, J., Xiao, L., and Li, X.: Does elevation-dependent warming hold true above 5000 m elevation? Lessons from the Tibetan Plateau, npj Clim Atmos Sci, 1, 1–7, https://doi.org/10.1038/s41612-018-0030-z, number: 1 Publisher: Nature Publishing Group, 2018.

González-Olabarria, J. R., Mola-Yudego, B., and Coll, L.: Different Factors for Different Causes: Analysis of the Spatial Aggregations of Fire Ignitions in Catalonia (Spain), Risk Analysis, 35, 1197–1209, https://doi.org/10.1111/risa.12339, _eprint: https://onlinelibrary.wiley.com/doi/pdf/10.1111/risa.12339, 2015.

Griffiths, A. D., Conen, F., Weingartner, E., Zimmermann, L., Chambers, S. D., Williams, A. G., and Steinbacher, M.: Surface-to-mountaintop transport characterised by radon observations at the Jungfraujoch, Atmospheric Chemistry and Physics, 14, 12 763–12 779, https://doi.org/10.5194/acp-14-12763-2014, publisher: Copernicus GmbH, 2014.

https://doi.org/10.5194/egusphere-2023-570
Preprint. Discussion started: 11 April 2023

Guo, Q., Hu, M., Guo, S., Wu, Z., Peng, J., and Wu, Y.: The variability in the relationship between black carbon and carbon monoxide over the eastern coast of China: BC aging during transport, Atmospheric Chemistry and Physics, 17, 10 395–10 403, https://doi.org/10.5194/acp-17-10395-2017, 2017.

Gysel, M., McFiggans, G. B., and Coe, H.: Inversion of tandem differential mobility analyser (TDMA) measurements, Journal of Aerosol Science, 40, 134–151, https://doi.org/https://doi.org/10.1016/j.jaerosci.2008.07.013, 2009.

Healy, R. M., Wang, J. M., Jeong, C.-H., Lee, A. K. Y., Willis, M. D., Jaroudi, E., Zimmerman, N., Hilker, N., Murphy, M., Eckhardt, S., Stohl, A., Abbatt, J. P. D., Wenger, J. C., and Evans, G. J.: Light-absorbing properties of ambient black carbon and brown carbon from fossil fuel and biomass burning sources, Journal of Geophysical Research: Atmospheres, 120, 6619–6633, https://doi.org/10.1002/2015JD023382, _eprint: https://onlinelibrary.wiley.com/doi/pdf/10.1002/2015JD023382, 2015.

Henne, S., Brunner, D., Folini, D., Solberg, S., Klausen, J., and Buchmann, B.: Assessment of parameters describing representativeness of air quality in-situ measurement sites, Atmospheric Chemistry and Physics, 10, 3561–3581, https://doi.org/10.5194/acp-10-3561-2010, publisher: Copernicus GmbH, 2010.

Herrmann, E., Weingartner, E., Henne, S., Vuilleumier, L., Bukowiecki, N., Steinbacher, M., Conen, F., Collaud Coen, M., Hammer, E., Jurányi, Z., Baltensperger, U., and Gysel, M.: Analysis of long-term aerosol size distribution data from Jungfraujoch with emphasis on free tropospheric conditions, cloud influence, and air mass transport, Journal of Geophysical Research: Atmospheres, 120, 9459–9480, https://doi.org/10.1002/2015JD023660, publisher: John Wiley & Sons, Ltd, 2015.

Hoyle, C. R., Webster, C. S., Rieder, H. E., Nenes, A., Hammer, E., Herrmann, E., Gysel, M., Bukowiecki, N., Weingartner, E., Steinbacher, M., and Baltensperger, U.: Chemical and physical influences on aerosol activation in liquid clouds: a study based on observations from the Jungfraujoch, Switzerland, Atmospheric Chemistry and Physics, 16, 4043–4061, https://doi.org/10.5194/acp-16-4043-2016, publisher: Copernicus GmbH, 2016.

Hulin, M., Gheusi, F., Lothon, M., Pont, V., Lohou, F., Ramonet, M., Delmotte, M., Derrien, S., Athier, G., Meyerfeld, Y., Bezombes, Y., Augustin, P., and Ravetta, F.: Observations of Thermally Driven Circulations in the Pyrenees: Comparison of Detection Methods and Impact on Atmospheric Composition Measured at a Mountaintop, Journal of Applied Meteorology and Climatology, 58, 717–740, https://doi.org/10.1175/JAMC-D-17-0268.1, publisher: American Meteorological Society Section: Journal of Applied Meteorology and Climatology, 2019.

Kanaya, Y., Pan, X., Miyakawa, T., Komazaki, Y., Taketani, F., Uno, I., and Kondo, Y.: Long-term observations of black carbon mass concentrations at Fukue Island, western Japan, during 2009–2015: constraining wet removal rates and emission strengths from East Asia, Atmospheric Chemistry and Physics, 16, 10 689–10 705, https://doi.org/10.5194/acp-16-10689-2016, publisher: Copernicus GmbH, 2016.

Kirchstetter, T. W., Novakov, T., and Hobbs, P. V.: Evidence that the spectral dependence of light absorption by aerosols is affected by organic carbon, Journal of Geophysical Research: Atmospheres, 109, https://doi.org/10.1029/2004JD004999, _eprint: https://onlinelibrary.wiley.com/doi/pdf/10.1029/2004JD004999, 2004.

Knox, A., Evans, G. J., Brook, J. R., Yao, X., Jeong, C.-H., Godri, K. J., Sabaliauskas, K., and Slowik, J. G.: Mass Absorption Cross-Section of Ambient Black Carbon Aerosol in Relation to Chemical Age, Aerosol Science and Technology, 43, 522–532, https://doi.org/10.1080/02786820902777207, publisher: Taylor & Francis _eprint: https://doi.org/10.1080/02786820902777207, 2009.

Ko, J., Krasowsky, T., and Ban-Weiss, G.: Measurements to determine the mixing state of black carbon emitted from the 2017–2018 California wildfires and urban Los Angeles, Atmospheric Chemistry and Physics, 20, 15 635–15 664, https://doi.org/10.5194/acp-20-15635-2020, publisher: Copernicus GmbH, 2020.

https://doi.org/10.5194/egusphere-2023-570
Preprint. Discussion started: 11 April 2023

Kondo, Y., Moteki, N., Oshima, N., Ohata, S., Koike, M., Shibano, Y., Takegawa, N., and Kita, K.: Effects of wet deposition on the abundance and size distribution of black carbon in East Asia, Journal of Geophysical Research: Atmospheres, 121, 4691–4712, https://doi.org/10.1002/2015JD024479, _eprint: https://agupubs.onlinelibrary.wiley.com/doi/pdf/10.1002/2015JD024479, 2016.

Krasowsky, T. S., McMeeking, G. R., Wang, D., Sioutas, C., and Ban-Weiss, G. A.: Measurements of the impact of atmospheric aging on physical and optical properties of ambient black carbon particles in Los Angeles, Atmospheric Environment, 142, 496–504, https://doi.org/10.1016/j.atmosenv.2016.08.010, 2016.

Laborde, M., Crippa, M., Tritscher, T., Jurányi, Z., Decarlo, P. F., Temime-Roussel, B., Marchand, N., Eckhardt, S., Stohl, A., Baltensperger, U., Prevot, A. S. H., Weingartner, E., and Gysel, M.: Black carbon physical properties and mixing state in the European megacity Paris, Atmospheric Chemistry and Physics, 13, 5831–5856, https://doi.org/10.5194/acp-13-5831-2013, publisher: European Geosciences Union, 2013.

Laj, P., Bigi, A., Rose, C., Andrews, E., Lund Myhre, C., Collaud Coen, M., Lin, Y., Wiedensohler, A., Schulz, M., Ogren, J. A., Fiebig, M., Gliß, J., Mortier, A., Pandolfi, M., Petäja, T., Kim, S.-W., Aas, W., Putaud, J.-P., Mayol-Bracero, O., Keywood, M., Labrador, L., Aalto, P., Ahlberg, E., Alados Arboledas, L., Alastuey, A., Andrade, M., Artíñano, B., Ausmeel, S., Arsov, T., Asmi, E., Backman, J., Baltensperger, U., Bastian, S., Bath, O., Beukes, J. P., Brem, B. T., Bukowiecki, N., Conil, S., Couret, C., Day, D., Dayantolis, W., Degorska, A., Eleftheriadis, K., Fetfatzis, P., Favez, O., Flentje, H., Gini, M. I., Gregorič, A., Gysel-Beer, M., Hallar, A. G., Hand, J., Hoffer, A., Hueglin, C., Hooda, R. K., Hyvärinen, A., Kalapov, I., Kalivitis, N., Kasper-Giebl, A., Kim, J. E., Kouvarakis, G., Kranjc, I., Krejci, R., Kulmala, M., Labuschagne, C., Lee, H.-J., Lihavainen, H., Lin, N.-H., Löschau, G., Luoma, K., Marinoni, A., Martins Dos Santos, S., Meinhardt, F., Merkel, M., Metzger, J.-M., Mihalopoulos, N., Nguyen, N. A., Ondracek, J., Pérez, N., Perrone, M. R., Petit, J.-E., Picard, D., Pichon, J.-M., Pont, V., Prats, N., Prenni, A., Reisen, F., Romano, S., Sellegri, K., Sharma, S., Schauer, G., Sheridan, P., Sherman, J. P., Schütze, M., Schwerin, A., Sohmer, R., Sorribas, M., Steinbacher, M., Sun, J., Titos, G., Toczko, B., Tuch, T., Tulet, P., Tunved, P., Vakkari, V., Velarde, F., Velasquez, P., Villani, P., Vratolis, S., Wang, S.-H., Weinhold, K., Weller, R., Yela, M., Yus-Diez, J., Zdimal, V., Zieger, P., and Zikova, N.: A global analysis of climate-relevant aerosol properties retrieved from the network of Global Atmosphere Watch (GAW) near-surface observatories, Atmospheric Measurement Techniques, 13, 4353–4392, https://doi.org/10.5194/amt-13-4353-2020, publisher: Copernicus GmbH, 2020.

Liu, C., Chung, C. E., Yin, Y., and Schnaiter, M.: The absorption Ångström exponent of black carbon: from numerical aspects, Atmospheric Chemistry and Physics, 18, 6259–6273, https://doi.org/10.5194/acp-18-6259-2018, publisher: Copernicus GmbH, 2018.

Liu, D., Flynn, M., Gysel, M., Targino, A., Crawford, I., Bower, K., Choularton, T., Jurányi, Z., Steinbacher, M., Hüglin, C., Curtius, J., Kampus, M., Petzold, A., Weingartner, E., Baltensperger, U., and Coe, H.: Single particle characterization of black carbon aerosols at a tropospheric alpine site in Switzerland, Atmospheric Chemistry and Physics, 10, 7389–7407, https://doi.org/10.5194/acp-10-7389-2010, publisher: Copernicus GmbH, 2010.

Liu, D., Ding, S., Zhao, D., Hu, K., Yu, C., Hu, D., Wu, Y., Zhou, C., Tian, P., Liu, Q., Wu, Y., Zhang, J., Kong, S., Huang, M., and Ding, D.: Black Carbon Emission and Wet Scavenging From Surface to the Top of Boundary Layer Over Beijing Region, Journal of Geophysical Research: Atmospheres, 125, e2020JD033 096, https://doi.org/10.1029/2020JD033096, _eprint: https://onlinelibrary.wiley.com/doi/pdf/10.1029/2020JD033096, 2020a.

Liu, F., Yon, J., Fuentes, A., Lobo, P., Smallwood, G. J., and Corbin, J. C.: Review of recent literature on the light absorption properties of black carbon: Refractive index, mass absorption cross section, and absorption function, Aerosol Science and Technology, 54, 33–51, https://doi.org/10.1080/02786826.2019.1676878, publisher: Taylor & Francis _eprint: https://doi.org/10.1080/02786826.2019.1676878, 2020b.

https://doi.org/10.5194/egusphere-2023-570
Preprint. Discussion started: 11 April 2023

Liu, H., Pan, X., Liu, D., Liu, X., Chen, X., Tian, Y., Sun, Y., Fu, P., and Wang, Z.: Mixing characteristics of refractory black carbon aerosols determined by a tandem CPMA-SP2 system at an urban site in Beijing, Atmospheric Chemistry and Physics Discussions, pp. 1–25, https://doi.org/10.5194/acp-2019-244, 2019.

Liu, S., Aiken, A. C., Gorkowski, K., Dubey, M. K., Cappa, C. D., Williams, L. R., Herndon, S. C., Massoli, P., Fortner, E. C., Chhabra, P. S., Brooks, W. A., Onasch, T. B., Jayne, J. T., Worsnop, D. R., China, S., Sharma, N., Mazzoleni, C., Xu, L., Ng, N. L., Liu, D., Allan, J. D., Lee, J. D., Fleming, Z. L., Mohr, C., Zotter, P., Szidat, S., and Prévôt, A. S. H.: Enhanced light absorption by mixed source black and brown carbon particles in UK winter, Nature Communications, 6, 8435, https://doi.org/10.1038/ncomms9435, 2015.

Liu, X., Cheng, Z., Yan, L., and Yin, Z.-Y.: Elevation dependency of recent and future minimum surface air temperature trends in the Tibetan Plateau and its surroundings, Global and Planetary Change, 68, 164–174, https://doi.org/10.1016/j.gloplacha.2009.03.017, 2009.

López-Moreno, J. I., El-Kenawy, A., Revuelto, J., Azorín-Molina, C., Morán-Tejeda, E., Lorenzo-Lacruz, J., Zabalza, J., and Vicente-Serrano, S. M.: Observed trends and future projections for winter warm events in the Ebro basin, northeast Iberian Peninsula, International Journal of Climatology, 34, 49–60, https://doi.org/10.1002/joc.3665, _eprint: https://rmets.onlinelibrary.wiley.com/doi/pdf/10.1002/joc.3665, 2014.

Mallet, M., Dubovik, O., Nabat, P., Dulac, F., Kahn, R., Sciare, J., Paronis, D., and Léon, J. F.: Absorption properties of Mediterranean aerosols obtained from multi-year ground-based remote sensing observations, Atmospheric Chemistry and Physics, 13, 9195–9210, https://doi.org/10.5194/acp-13-9195-2013, publisher: Copernicus GmbH, 2013.

Marenco, A., Gouget, H., Nédélec, P., Pagés, J.-P., and Karcher, F.: Evidence of a long-term increase in tropospheric ozone from Pic du Midi data series: Consequences: Positive radiative forcing, Journal of Geophysical Research: Atmospheres, 99, 16 617–16 632, https://onlinelibrary.wiley.com/doi/abs/10.1029/94JD00021, publisher: John Wiley & Sons, Ltd, 1994.

Marusczak, N., Sonke, J. E., Fu, X., and Jiskra, M.: Tropospheric GOM at the Pic du Midi Observatory—Correcting Bias in Denuder Based Observations, Environ. Sci. Technol., 51, 863–869, https://doi.org/10.1021/acs.est.6b04999, publisher: American Chemical Society, 2017.

Matsui, H., Hamilton, D. S., and Mahowald, N. M.: Black carbon radiative effects highly sensitive to emitted particle size when resolving mixing-state diversity, Nat Commun, 9, 3446, https://doi.org/10.1038/s41467-018-05635-1, number: 1 Publisher: Nature Publishing Group, 2018.

McMeeking, G. R., Hamburger, T., Liu, D., Flynn, M., Morgan, W. T., Northway, M., Highwood, E. J., Krejci, R., Allan, J. D., Minikin, A., and Coe, H.: Black carbon measurements in the boundary layer over western and northern Europe, Atmospheric Chemistry and Physics, 10, 9393–9414, https://doi.org/10.5194/acp-10-9393-2010, 2010.

McMeeking, G. R., Fortner, E., Onasch, T. B., Taylor, J. W., Flynn, M., Coe, H., and Kreidenweis, S. M.: Impacts of nonrefractory material on light absorption by aerosols emitted from biomass burning, Journal of Geophysical Research: Atmospheres, 119, 12,272–12,286, https://doi.org/10.1002/2014JD021750, _eprint: https://agupubs.onlinelibrary.wiley.com/doi/pdf/10.1002/2014JD021750, 2014.

Moteki, N. and Kondo, Y.: Effects of Mixing State on Black Carbon Measurements by Laser-Induced Incandescence, null, 41, 398–417, https://doi.org/10.1080/02786820701199728, publisher: Taylor & Francis, 2007.

Moteki, N., Kondo, Y., Oshima, N., Takegawa, N., Koike, M., Kita, K., Matsui, H., and Kajino, M.: Size dependence of wet removal of black carbon aerosols during transport from the boundary layer to the free troposphere, Geophysical Research Letters, 39, https://doi.org/10.1029/2012GL052034, _eprint: https://onlinelibrary.wiley.com/doi/pdf/10.1029/2012GL052034, 2012.

Motos, G., Schmale, J., Corbin, J. C., Modini, R. L., Karlen, N., Bertò, M., Baltensperger, U., and Gysel-Beer, M.: Cloud droplet activation properties and scavenged fraction of black carbon in liquid-phase clouds at the high-alpine research station Jungfraujoch

https://doi.org/10.5194/egusphere-2023-570
Preprint. Discussion started: 11 April 2023

(3580 m a.s.l.), Atmospheric Chemistry and Physics, 19, 3833–3855, https://doi.org/10.5194/acp-19-3833-2019, publisher: Copernicus GmbH, 2019.

Motos, G., Corbin, J. C., Schmale, J., Modini, R. L., Bertò, M., Kupiszewski, P., Baltensperger, U., and Gysel-Beer, M.: Black Carbon Aerosols in the Lower Free Troposphere are Heavily Coated in Summer but Largely Uncoated in Winter at Jungfraujoch in the Swiss Alps, Geophysical Research Letters, 47, e2020GL088 011, https://doi.org/10.1029/2020GL088011, publisher: John Wiley & Sons, Ltd, 2020.

Myhre, G. and Samset, B. H.: Standard climate models radiation codes underestimate black carbon radiative forcing, Atmospheric Chemistry and Physics, 15, 2883–2888, https://doi.org/10.5194/acp-15-2883-2015, 2015.

Müller, T., Laborde, M., Kassell, G., and Wiedensohler, A.: Design and performance of a three-wavelength LED-based total scatter and backscatter integrating nephelometer, Atmospheric Measurement Techniques, 4, 1291–1303, https://doi.org/10.5194/amt-4-1291-2011, publisher: Copernicus GmbH, 2011.

Nessler, R., Bukowiecki, N., Henning, S., Weingartner, E., Calpini, B., and Baltensperger, U.: Simultaneous dry and ambient measurements of aerosol size distributions at the Jungfraujoch, Tellus Series B Chemical and Physical Meteorology B, 55, 808–819, https://doi.org/10.1034/j.1600-0889.2003.00067.x, aDS Bibcode: 2003TellB..55..808N, 2003.

Ohata, S., Schwarz, J. P., Moteki, N., Koike, M., Takami, A., and Kondo, Y.: Hygroscopicity of materials internally mixed with black carbon measured in Tokyo, Journal of Geophysical Research: Atmospheres, 121, 362–381, https://doi.org/https://doi.org/10.1002/2015JD024153, _eprint: https://onlinelibrary.wiley.com/doi/pdf/10.1002/2015JD024153, 2016.

Pan, X. L., Kanaya, Y., Wang, Z. F., Liu, Y., Pochanart, P., Akimoto, H., Sun, Y. L., Dong, H. B., Li, J., Irie, H., and Takigawa, M.: Correlation of black carbon aerosol and carbon monoxide in the high-altitude environment of Mt. Huang in Eastern China, Atmospheric Chemistry and Physics, 11, 9735–9747, https://doi.org/10.5194/acp-11-9735-2011, publisher: Copernicus GmbH, 2011.

Pandolfi, M., Ripoll, A., Querol, X., and Alastuey, A.: Climatology of aerosol optical properties and black carbon mass absorption cross section at a remote high-altitude site in the western Mediterranean Basin, Atmospheric Chemistry and Physics, 14, 6443–6460, https://doi.org/10.5194/acp-14-6443-2014, publisher: Copernicus GmbH, 2014.

Pandolfi, M., Alados-Arboledas, L., Alastuey, A., Andrade, M., Angelov, C., Artiñano, B., Backman, J., Baltensperger, U., Bonasoni, P., Bukowiecki, N., Collaud Coen, M., Conil, S., Coz, E., Crenn, V., Dudoitis, V., Ealo, M., Eleftheriadis, K., Favez, O., Fetfatzis, P., Fiebig, M., Flentje, H., Ginot, P., Gysel, M., Henzing, B., Hoffer, A., Holubova Smejkalova, A., Kalapov, I., Kalivitis, N., Kouvarakis, G., Kristensson, A., Kulmala, M., Lihavainen, H., Lunder, C., Luoma, K., Lyamani, H., Marinoni, A., Mihalopoulos, N., Moerman, M., Nicolas, J., O'Dowd, C., Petäjä, T., Petit, J.-E., Pichon, J. M., Prokopciuk, N., Putaud, J.-P., Rodríguez, S., Sciare, J., Sellegri, K., Swietlicki, E., Titos, G., Tuch, T., Tunved, P., Ulevicius, V., Vaishya, A., Vana, M., Virkkula, A., Vratolis, S., Weingartner, E., Wiedensohler, A., and Laj, P.: A European aerosol phenomenology – 6: scattering properties of atmospheric aerosol particles from 28 ACTRIS sites, Atmospheric Chemistry and Physics, 18, 7877–7911, https://doi.org/10.5194/acp-18-7877-2018, publisher: Copernicus GmbH, 2018.

Peng, J., Hu, M., Guo, S., Du, Z., Zheng, J., Shang, D., Levy Zamora, M., Zeng, L., Shao, M., Wu, Y.-S., Zheng, J., Wang, Y., Glen, C. R., Collins, D. R., Molina, M. J., and Zhang, R.: Markedly enhanced absorption and direct radiative forcing of black carbon under polluted urban environments, Proceedings of the National Academy of Sciences, 113, 4266–4271, https://doi.org/10.1073/pnas.1602310113, publisher: Proceedings of the National Academy of Sciences, 2016.

Pepin, N., Bradley, R. S., Diaz, H. F., Baraer, M., Caceres, E. B., Forsythe, N., Fowler, H., Greenwood, G., Hashmi, M. Z., Liu, X. D., Miller, J. R., Ning, L., Ohmura, A., Palazzi, E., Rangwala, I., Schöner, W., Severskiy, I., Shahgedanova, M., Wang, M. B., Williamson, S. N.,

https://doi.org/10.5194/egusphere-2023-570
Preprint. Discussion started: 11 April 2023

Yang, D. Q., and Mountain Research Initiative EDW Working Group: Elevation-dependent warming in mountain regions of the world, Nature Clim Change, 5, 424–430, https://doi.org/10.1038/nclimate2563, number: 5 Publisher: Nature Publishing Group, 2015.

Pepin, N., Deng, H., Zhang, H., Zhang, F., Kang, S., and Yao, T.: An Examination of Temperature Trends at High Elevations Across the Tibetan Plateau: The Use of MODIS LST to Understand Patterns of Elevation-Dependent Warming, Journal of Geophysical Research: Atmospheres, 124, 5738–5756, https://doi.org/10.1029/2018JD029798, _eprint: https://onlinelibrary.wiley.com/doi/pdf/10.1029/2018JD029798, 2019.

Petetin, H., Sauvage, B., Parrington, M., Clark, H., Fontaine, A., Athier, G., Blot, R., Boulanger, D., Cousin, J.-M., Nédélec, P., and Thouret, V.: The role of biomass burning as derived from the tropospheric CO vertical profiles measured by IAGOS aircraft in 2002–2017, Atmospheric Chemistry and Physics, 18, 17 277–17 306, https://doi.org/10.5194/acp-18-17277-2018, publisher: Copernicus GmbH, 2018.

Rangwala, I.: Amplified water vapour feedback at high altitudes during winter, International Journal of Climatology, 33, 897–903, https://doi.org/10.1002/joc.3477, _eprint: https://onlinelibrary.wiley.com/doi/pdf/10.1002/joc.3477, 2013.

Réveillet, M., Dumont, M., Gascoin, S., Lafaysse, M., Nabat, P., Ribes, A., Nheili, R., Tuzet, F., Ménégoz, M., Morin, S., Picard, G., and Ginoux, P.: Black carbon and dust alter the response of mountain snow cover under climate change, Nat Commun, 13, 5279, https://doi.org/10.1038/s41467-022-32501-y, number: 1 Publisher: Nature Publishing Group, 2022.

Samset, B. H. and Myhre, G.: Climate response to externally mixed black carbon as a function of altitude, Journal of Geophysical Research: Atmospheres, 120, 2913–2927, https://doi.org/10.1002/2014JD022849, _eprint: https://onlinelibrary.wiley.com/doi/pdf/10.1002/2014JD022849, 2015.

Sanroma, E., Palle, E., and Sanchez-Lorenzo, A.: Long-term changes in insolation and temperatures at different altitudes, Environ. Res. Lett., 5, 024 006, https://doi.org/10.1088/1748-9326/5/2/024006, 2010.

Schill, G. P., Froyd, K. D., Bian, H., Kupc, A., Williamson, C., Brock, C. A., Ray, E., Hornbrook, R. S., Hills, A. J., Apel, E. C., Chin, M., Colarco, P. R., and Murphy, D. M.: Widespread biomass burning smoke throughout the remote troposphere, Nat. Geosci., 13, 422–427, https://doi.org/10.1038/s41561-020-0586-1, number: 6 Publisher: Nature Publishing Group, 2020.

Schwarz, J. P., Gao, R. S., Fahey, D. W., Thomson, D. S., Watts, L. A., Wilson, J. C., Reeves, J. M., Darbeheshti, M., Baumgardner, D. G., Kok, G. L., Chung, S. H., Schulz, M., Hendricks, J., Lauer, A., Kärcher, B., Slowik, J. G., Rosenlof, K. H., Thompson, T. L., Langford, A. O., Loewenstein, M., and Aikin, K. C.: Single-particle measurements of midlatitude black carbon and light-scattering aerosols from the boundary layer to the lower stratosphere, Journal of Geophysical Research: Atmospheres, 111, https://doi.org/https://doi.org/10.1029/2006JD007076, _eprint: https://onlinelibrary.wiley.com/doi/pdf/10.1029/2006JD007076, 2006.

Schwarz, J. P., Spackman, J. R., Fahey, D. W., Gao, R. S., Lohmann, U., Stier, P., Watts, L. A., Thomson, D. S., Lack, D. A., Pfister, L., Mahoney, M. J., Baumgardner, D., Wilson, J. C., and Reeves, J. M.: Coatings and their enhancement of black carbon light absorption in the tropical atmosphere, Journal of Geophysical Research: Atmospheres, 113, https://doi.org/10.1029/2007JD009042, publisher: John Wiley & Sons, Ltd, 2008.

Schwarz, J. P., Spackman, J. R., Gao, R. S., Perring, A. E., Cross, E., Onasch, T. B., Ahern, A., Wrobel, W., Davidovits, P., Olfert, J., Dubey, M. K., Mazzoleni, C., and Fahey, D. W.: The Detection Efficiency of the Single Particle Soot Photometer, Aerosol Science and Technology, 44, 612–628, https://doi.org/10.1080/02786826.2010.481298, publisher: Taylor & Francis _eprint: https://doi.org/10.1080/02786826.2010.481298, 2010.

Sedlacek, A. J. I., Lewis, E. R., Onasch, T. B., Zuidema, P., Redemann, J., Jaffe, D., and Kleinman, L. I.: Using the Black Carbon Particle Mixing State to Characterize the Lifecycle of Biomass Burning Aerosols, Environ. Sci. Technol., 56, 14 315–14 325, https://doi.org/10.1021/acs.est.2c03851, publisher: American Chemical Society, 2022.

https://doi.org/10.5194/egusphere-2023-570
Preprint. Discussion started: 11 April 2023

Shiraiwa, M., Kondo, Y., Moteki, N., Takegawa, N., Sahu, L. K., Takami, A., Hatakeyama, S., Yonemura, S., and Blake, D. R.: Radiative impact of mixing state of black carbon aerosol in Asian outflow, Journal of Geophysical Research: Atmospheres, 113, https://doi.org/10.1029/2008JD010546, _eprint: https://agupubs.onlinelibrary.wiley.com/doi/pdf/10.1029/2008JD010546, 2008.

Spackman, J. R., Gao, R. S., Neff, W. D., Schwarz, J. P., Watts, L. A., Fahey, D. W., Holloway, J. S., Ryerson, T. B., Peischl, J., and Brock, C. A.: Aircraft observations of enhancement and depletion of black carbon mass in the springtime Arctic, Atmospheric Chemistry and Physics, 10, 9667–9680, https://doi.org/10.5194/acp-10-9667-2010, 2010.

Sun, J., Hermann, M., Yuan, Y., Birmili, W., Collaud Coen, M., Weinhold, K., Madueño, L., Poulain, L., Tuch, T., Ries, L., Sohmer, R., Couret, C., Frank, G., Brem, B. T., Gysel-Beer, M., Ma, N., and Wiedensohler, A.: Long-term trends of black carbon and particle number concentration in the lower free troposphere in Central Europe, Environmental Sciences Europe, 33, 47, https://doi.org/10.1186/s12302-021-00488-w, 2021.

Szopa, S., Naik, V., Adhikary, B., Artaxo, P., Berntsen, T., Collins, W., Fuzzi, S., Gallardo, L., Kiendler-Scharr, A., Klimont, Z., Liao, H., Unger, N., Zanis, P., and Kuo, C.: Short-Lived Climate Forcers, in: AGU Fall Meeting Abstracts, vol. 2021, pp. U13B–06, 2021a.

Szopa, S., Naik, V., Adhikary, b., Artaxo, P., Berntsen, T., Collins, W. D., Fuzzi, S., Gallardo, L., Kiendler-Scharr, A., Klimont, Z., Liao, H., Unger, N., and Zanis, P.: Short-Lived Climate Forcers, in: Climate Change 2021: The Physical Science Basis. Contribution of Working Group I to the Sixth Assessment Report of the Intergovernmental Panel on Climate Change, edited by Press, C. U., pp. 817–922, Cambridge, United Kingdom and New York, NY, USA, https://doi.org/10.1017/9781009157896.008, 2021b.

Taylor, J. W., Allan, J. D., Allen, G., Coe, H., Williams, P. I., Flynn, M. J., Le Breton, M., Muller, J. B. A., Percival, C. J., Oram, D., Forster, G., Lee, J. D., Rickard, A. R., Parrington, M., and Palmer, P. I.: Size-dependent wet removal of black carbon in Canadian biomass burning plumes, Atmospheric Chemistry and Physics, 14, 13 755–13 771, https://doi.org/10.5194/acp-14-13755-2014, 2014.

Tsamalis, C., Ravetta, F., Gheusi, F., Delbarre, H., and Augustin, P.: Mixing of free-tropospheric air with the lowland boundary layer during anabatic transport to a high altitude station, Atmospheric Research, 143, 425–437, https://doi.org/10.1016/j.atmosres.2014.03.011, 2014.

Van de Hulst, H.: Light scattering by small particles, John Wiley & Sons, Chapman & Hall, New York, 1957.

Venzac, H., Sellegri, K., Villani, P., Picard, D., and Laj, P.: Seasonal variation of aerosol size distributions in the free troposphere and residual layer at the puy de Dôme station, France, Atmospheric Chemistry and Physics, 9, 1465–1478, https://doi.org/10.5194/acp-9-1465-2009, publisher: Copernicus GmbH, 2009.

Wang, Q., Huang, R., Zhao, Z., Cao, J., Ni, H., Tie, X., Zhu, C., Shen, Z., Wang, M., Dai, W., Han, Y., Zhang, N., and Prévôt, A. S. H.: Effects of photochemical oxidation on the mixing state and light absorption of black carbon in the urban atmosphere of China, Environ. Res. Lett., 12, 044 012, https://doi.org/10.1088/1748-9326/aa64ea, publisher: IOP Publishing, 2017.

Whiteman, C. D.: Mountain meteorology: fundamentals and applications, New York, Oxford, oxford university press edn., 2000.

Whittlestone, S. and Zahorowski, W.: Baseline radon detectors for shipboard use: Development and deployment in the First Aerosol Characterization Experiment (ACE 1), Journal of Geophysical Research: Atmospheres, 103, 16 743–16 751, https://doi.org/10.1029/98JD00687, _eprint: https://onlinelibrary.wiley.com/doi/pdf/10.1029/98JD00687, 1998.

Wong, J. P. S., Tsagkaraki, M., Tsiodra, I., Mihalopoulos, N., Violaki, K., Kanakidou, M., Sciare, J., Nenes, A., and Weber, R. J.: Atmospheric evolution of molecular-weight-separated brown carbon from biomass burning, Atmospheric Chemistry and Physics, 19, 7319–7334, https://doi.org/10.5194/acp-19-7319-2019, publisher: Copernicus GmbH, 2019.

Xie, C., Xu, W., Wang, J., Liu, D., Ge, X., Zhang, Q., Wang, Q., Du, W., Zhao, J., Zhou, W., Li, J., Fu, P., Wang, Z., Worsnop, D., and Sun, Y.: Light absorption enhancement of black carbon in urban Beijing in summer, Atmospheric Environment, 213, 499–504, https://doi.org/10.1016/j.atmosenv.2019.06.041, 2019.

https://doi.org/10.5194/egusphere-2023-570
Preprint. Discussion started: 11 April 2023

Xu, X., Zhao, W., Qian, X., Wang, S., Fang, B., Zhang, Q., Zhang, W., Venables, D. S., Chen, W., Huang, Y., Deng, X., Wu, B., Lin, X., Zhao, S., and Tong, Y.: The influence of photochemical aging on light absorption of atmospheric black carbon and aerosol single-scattering albedo, Atmospheric Chemistry and Physics, 18, 16 829–16 844, https://doi.org/https://doi.org/10.5194/acp-18-16829-2018, publisher: Copernicus GmbH, 2018.

Yus-Díez, J., Via, M., Alastuey, A., Karanasiou, A., Minguillón, M. C., Perez, N., Querol, X., Reche, C., Ivančič, M., Rigler, M., and Pandolfi, M.: Absorption enhancement of black carbon particles in a Mediterranean city and countryside: effect of particulate matter chemistry, ageing and trend analysis, Atmospheric Chemistry and Physics, 22, 8439–8456, https://doi.org/10.5194/acp-22-8439-2022, publisher: Copernicus GmbH, 2022.

Zanatta, M., Gysel, M., Bukowiecki, N., Müller, T., Weingartner, E., Areskoug, H., Fiebig, M., Yttri, K., Mihalopoulos, N., Kouvarakis, G., Beddows, D., Harrison, R., Cavalli, F., Putaud, J., Spindler, G., Wiedensohler, A., Alastuey, A., Pandolfi, M., Sellegri, K., Swietlicki, E., Jaffrezo, J., Baltensperger, U., and Laj, P.: A European aerosol phenomenology-5: Climatology of black carbon optical properties at 9 regional background sites across Europe, Atmospheric Environment, 145, 346–364, https://doi.org/10.1016/j.atmosenv.2016.09.035, 2016.

Zeng, L., Zhang, A., Wang, Y., Wagner, N. L., Katich, J. M., Schwarz, J. P., Schill, G. P., Brock, C., Froyd, K. D., Murphy, D. M., Williamson, C. J., Kupc, A., Scheuer, E., Dibb, J., and Weber, R. J.: Global Measurements of Brown Carbon and Estimated Direct Radiative Effects, Geophysical Research Letters, 47, e2020GL088 747, https://doi.org/10.1029/2020GL088747, _eprint: https://agupubs.onlinelibrary.wiley.com/doi/pdf/10.1029/2020GL088747, 2020.

Zhang, Y., Favez, O., Canonaco, F., Liu, D., Močnik, G., Amodeo, T., Sciare, J., Prévôt, A. S. H., Gros, V., and Albinet, A.: Evidence of major secondary organic aerosol contribution to lensing effect black carbon absorption enhancement, npj Clim Atmos Sci, 1, 1–8, https://doi.org/10.1038/s41612-018-0056-2, number: 1 Publisher: Nature Publishing Group, 2018.

Zhang, Y., Liu, H., Lei, S., Xu, W., Tian, Y., Yao, W., Liu, X., Liao, Q., Li, J., Chen, C., Sun, Y., Fu, P., Xin, J., Cao, J., Pan, X., and Wang, Z.: Mixing state of refractory black carbon in fog and haze at rural sites in winter on the North China Plain, Atmos. Chem. Phys., 21, 17 631–17 648, https://doi.org/10.5194/acp-21-17631-2021, 2021.

Zhu, C., Kanaya, Y., Yoshikawa-Inoue, H., Irino, T., Seki, O., and Tohjima, Y.: Sources of atmospheric black carbon and related carbonaceous components at Rishiri Island, Japan: The roles of Siberian wildfires and of crop residue burning in China, Environmental Pollution, 247, 55–63, https://doi.org/10.1016/j.envpol.2019.01.003, 2019.